METEOROLOGICAL CONDITIONS AND ANOMALIES DURING INTEX-NA

Henry E. Fuelberg
Michael J. Porter
Christopher M. Kiley
Danielle Morse

Department of Meteorology
Florida State University
Tallahassee, Florida USA

Submitted to

Journal of Geophysical Research--Atmospheres
INTEX Special Section

Index Terms:
0300 Atmospheric Composition and Structure
0368 Troposphere: Constituent Transport and Chemistry
3364 Synoptic Scale Meteorology
3324 Lightning

H.E. Fuelberg, M. J. Porter, C.M. Kiley, and D. Morse, Department of Meteorology, Florida State University, Tallahassee, FL 32306-4520, USA. (fuelberg@met.fsu.edu; mporter@met.fsu.edu; ckiley@met.fsu.edu; dmorse@met.fsu.edu)

June 2006

Abstract

Meteorological conditions are described during the Intercontinental Chemical Transport Experiment—North America (INTEX-NA) that was conducted over the United States during July and August 2004. Relatively zonal flow dominated the contiguous U.S. during the first two weeks of the mission, while a series of large amplitude troughs traversed the eastern half of the country during the final four weeks. These troughs were accompanied by cold fronts reaching the Gulf of Mexico—an uncommon occurrence during August. Frontal passages over the Northeast were somewhat above average, but the short time interval between passages precluded the formation of stagnant high pressure centers containing abundant pollution. Atmospheric chemistry during INTEX-NA was heavily influenced by record breaking fires over Alaska and western Canada. Persistent high pressure over Alaska provided ideal conditions for the wildfires and for transporting their burning by-products southeastward toward the INTEX domain where they were sampled by INTEX aircraft. Forward trajectories and satellite imagery showed that the plumes later were carried to parts of Europe, Africa, and even the Arctic. Deep convection and lightning were important factors during INTEX-NA. Cloud-to-ground (CG) lightning data show that horizontal patterns and numbers of lightning flashes during INTEX-NA are similar to those of 2003 and 2005. Statistics derived from 10 day backward trajectories indicate that the DC-8 sampled lightning influenced air ~ 65% of the time. If convection derived from the GFS meteorological model is considered, the DC-8 sampled convectively influenced air ~92% of the time, with many of these encounters occurring within 6 h of in situ sampling.

1. Introduction

The Intercontinental Chemical Transport Experiment—North America (INTEX-NA) was conducted over the contiguous United States and adjacent areas during July and August 2004 [*Singh et al.*, 2006] as part of NASA's Global Tropospheric Experiment (GTE) [*McNeal et al.,* 1984]. INTEX-NA was a component of the International Consortium for Atmospheric Research on Transport and Transformation (ICARTT) whose goals were to execute a series of coordinated experiments to study the emissions of aerosols and ozone precursors, as well as their chemical transformations and removal during transport to and over the North Atlantic Ocean [*Fehsenfeld et al.*, 2006]. The specific goals of INTEX-NA were 1) to understand the transport and transformation of gases and aerosols on transcontinental and intercontinental scales and their impact on air quality and climate, 2) quantify and characterize the inflow and outflow of pollution over North America, and 3) provide validation of ongoing satellite measurement programs such as Terra, Aura, and Envisat [*Singh et al.*, 2006].

Meteorological conditions play an important role in determining the transport and distribution of many chemical species [e.g., *Merrill et al.*, 1997; *Fuelberg et al.*, 2003]. For example, atmospheric temperature and humidity affect chemical reaction rates and thereby influence the lifetimes of many species [e.g., *Mauzerall et al.*, 1998; *Blake et al.*, 2001; *Martin et al.*, 2002]. Precipitation can scavenge some species (e.g., *Cohan et al.* [1999], *O'Sullivan et al.* [1999]), while lightning can create species such as nitrogen oxides [e.g., *Lawrence et al.*, 1994; *Bond et al.,* 2001]. Deep convection and smaller scale turbulent mixing transport surface-based species into the free troposphere where they can be carried vast distances by strong upper-level winds [e.g., *Maloney et al.,*

2001]. In addition, phases in the El Nino-Southern Oscillation (ENSO) can alter large scale transport patterns [e.g., *Trenberth et al*., 1997].

This paper describes the meteorological setting for INTEX-NA, including large-scale flow patterns, their departures from climatology, distributions of lightning, as well as several unusual aspects of the period, e.g., widespread wild fires over Alaska and Canada, and summer cold fronts reaching the United States Gulf Coast. The overall goal is to assess the representativeness of INTEX-NA with respect to typical summertime conditions and thereby facilitate the interpretation of the INTEX chemical data.

2. Data and Methodologies

INTEX-NA employed NASA's DC-8 flying laboratory to collect extensive in situ chemical and meteorological data. The eighteen science flights stretched from the eastern Pacific Ocean to the central Atlantic Ocean, and from southeastern Canada to the U.S. Gulf Coast [*Singh et al.*, 2006]. In addition, the Jetstream 31 (J31) aircraft flew over the Gulf of Maine with the goals of validating satellite retrievals of aerosol optical depth spectra and of water vapor columns, as well as measuring aerosol effects on radiative energy fluxes [*Russell et al*., 2006]. Although this paper focuses on the INTEX flight domain, it also considers various upwind and downwind regions whose meteorology affected the INTEX domain.

Our meteorological products were derived from reanalysis data prepared by the National Centers for Environmental Prediction (NCEP) [*Kalnay et al.,* 1996] and available on the web site of the NOAA-CIRES Climate Diagnostics Center (CDC) at URL http://www.cdc.noaa.gov. The data used to prepare our trajectories were from the

National Weather Service's Global Forecast System (GFS) which is a global spectral forecast model. Details about the current version of the GFS is available at http://www.emc.ncep.noaa.gov/modelinfo/index.html. Data were available four times daily (0000, 0600, 1200, and 1800 UTC) with a T254 spherical harmonic triangular truncation, interpolated to a 1.0^{o} x 1.0^{o} latitude-longitude horizontal grid. The vertical resolution includes 64 unequally-spaced sigma levels. For a surface pressure of 1000 hPa, 15 levels of these levels are below 800 hPa.

Trajectories were calculated using a kinematic model, i.e., employing u, v, and w wind components from the NCEP analyses. Additional details about our trajectory model are given in *Fuelberg et al.* [1996, 1999, 2000] and *Martin et al.* [2002]. Compared to earlier versions of the model, the current trajectories were not terminated if they intersected the lower boundary, but instead continued isobarically along the surface and possibly were lofted later by vertical motion, a procedure similar to *Stohl et al.* [1995]. Another important difference is that the advection scheme now is iterative over a 5 min interval, creating more precise trajectories. Limitations of trajectories are described by *Fuelberg et al*. [2000], *Maloney et al*. [2001], *Stohl* [1998], and *Stohl et al*. [1995].

Lightning data used in the study are from the National Lightning Detection Network (NLDN) that is owned and operated by Vaisala Inc. Specifics about the network's operations and methodology are discussed by *Cummins et al.* (1998). The network determines the location, time, and other characteristics of each cloud-to-ground (CG) flash. The detection efficiency and location accuracy of the NLDN have improved substantially since its inception in 1989. The latest system upgrade occurred during 2002. The network's current detection efficiency is 90-95%, and location is accurate to

94 within 500 m over most of the country [*Cummins et al.*, 2006]. No corrections were
95 applied to the data to compensate for variations in detection efficiency and location
96 accuracy across the study area. This produces an underestimation of flash counts. Weak
97 positive flashes (< 15 kA) were deleted from the data set since they are thought to
98 represent intra-cloud discharges. There currently is no way to detect total lightning
99 (cloud-to-ground plus intra-cloud) over the total U.S. on a continuous basis.
100

101 **3. Mission-Averaged Flow Patterns**

102 Mission-averaged flow patterns describe the overall conditions that influenced
103 transport during INTEX-NA. Figure 1 contains time-averaged data for the entire INTEX
104 period (July 1 – August 15, 2004). The sea level pressure analysis (Figure 1c) shows
105 well developed subtropical anticyclones off the east and west coasts of the U.S. With
106 central pressures of ~1024 hPa, they are semi-permanent features that exhibit little day-
107 to-day fluctuations in strength or location. However, Figure 1f shows that the extension
108 of the Bermuda High over the Southeast U.S. is ~ 3 hPa weaker during INTEX than the
109 long term climatological average (1968-1996). Later sections will show that this
110 characteristic of the Bermuda High had important implications for transport during
111 INTEX. The Pacific anticyclone also is slightly weaker than normal. There are no quasi-
112 permanent pressure centers over the land mass of North America during the composite
113 INTEX period. Instead, the next section will show that there were numerous important
114 transient systems that cancelled each other during the averaging procedure.
115 The time averaged height analysis at 500 hPa (~18,000 ft) (Figure 1b) contains
116 the two subtropical anticyclones seen at the surface. In addition, a low pressure trough is

117 oriented along the eastern U.S., and a high pressure ridge extends from the desert
118 southwest into Alaska. The East Coast trough is ~40 m more intense than the
119 climatological mean (Figure 1e), while the ridge over Alaska is ~70 m stronger than
120 average. Finally, the closed low off the west coast of Canada is ~15 m more intense than
121 typical. Since winds above the boundary layer blow approximately parallel to the height
122 contours with higher heights to the right of the winds, Figure 1b reveals that the central
123 U.S. on average experienced mid-tropospheric flow from the northwest, thereby
124 transporting air from Alaska and northwest Canada, while the eastern U.S. most often had
125 flow from the southwest. Other implications of the height pattern are described in later
126 sections.

127 Figure 1a shows time averaged vector winds and isotachs at 250 hPa (~ 34,000
128 ft). The mean position of the subtropical jet stream is from near Hawaii to the West
129 Coast. Greatest mean speeds are ~10 m s^{-1}. The polar jet, located farther north, has two
130 branches—one located just south of Alaska, with the second extending from extreme
131 northern Alaska to Hudson Bay. These two branches merge near Maine and then stretch
132 over the North Atlantic Ocean. Greatest mean wind speeds in both branches reach ~15 m
133 s^{-1}. As expected, wind directions at 250 hPa are similar to those below (Figures 1a-b).
134 The anomaly analysis (Figure 1d) reveals that the subtropical jet stream and southern
135 branch of the polar jet are near their climatological locations. However, the northern
136 branch of the polar jet is somewhat stronger (~7 m s^{-1}) than normal.

137

138 **4. Variability in Flow Patterns**

139 The Summer 2004 INTEX-NA period was unusual in several respects. Most of
140 the contiguous U.S. was colder than normal, several cold fronts extended as far south as

the Gulf Coast and central Florida, and Alaska was dominated by high pressure that caused excessive lightning and a large number of wildfires whose influence was detected during many INTEX flights. These meteorological aspects are described in the following sections.

4.1 Unusually Cool Summer Conditions

Figure 2 contains a series of 500 hPa (~18,000 ft) height analyses that document the evolution of middle tropospheric flow during INTEX-NA. The first fourteen days of INTEX (July 1-14, 2004) included five DC-8 science flights, three of which correspond to the panels in Figure 2 (Flights 3, 4, and 7 on July 1, 6, and 12, respectively). These first two weeks are characterized by a series of short wave troughs and ridges that travel from west to east across the contiguous U.S. (Figure 2a-c). A time vs. longitude plot of 500 hPa heights at 40^{o} N (Figure 3) shows the progression of these waves across the region. This procession of troughs and ridges generally brought alternating periods of southwesterly and northwesterly middle tropospheric flow as they passed a location. The time averaged 500 hPa analysis during the two week period (Figure 4a) shows high pressure over the South, and nearly zonal flow over the remainder of the country. Height anomalies during the period (Figure 4 b) generally are negative, but not excessively so (not more than -15 m). At the surface (not shown), the middle latitude systems were associated with cold fronts that carried polar air into the northern half of the U.S.

The remainder of the INTEX period (July 15 – August 15) exhibited greater anomalies, both at the surface and aloft. Figure 2d-h shows 500 hPa height fields on five of the thirteen remaining DC-8 flight days (Flight 9 on July 18, Flight 12 on July 25, Flight 14 on July 31, Flight 16 on August 6, and Flight 19 on August 13). An important

feature is the strength of the low pressure troughs over the eastern U.S. These troughs are especially impressive on July 18, August 6, and August 13 (Figure 2 d, g, and h) when they extend as far south as the central Gulf of Mexico. The systems also are clearly depicted in the time-longitude plot (Figure 3). The 500 hPa time-averaged height pattern (Figure 4c) shows the trough along the eastern U.S. and a ridge along the west coast, similar to that observed during the entire six week period (Figure 1b). This series of large amplitude waves is unusual for summer. Height anomalies on individual days are as much as 200 m less than the norm, and as much as 60 m below normal for the month long period (Figure 4d). Typical summertime wave patterns exhibit smaller amplitudes that do not reach as far south. The high pressure ridge along the west now is much stronger than during the first two weeks of INTEX. Later sections will show that this flow pattern was ideal for transporting smoke from wildfires in Alaska and northwestern Canada.

Cold frontal passages over the East and Gulf Coasts were more frequent than normal during INTEX-NA. Table 1 gives the number of cold fronts that passed the northeast U.S. near Boston, as well as those passing the Southeast near Atlanta between July 1 - August 15 of years 2000-2005. Frontal locations were obtained from the National Weather Service's archive of Daily Weather Maps http://docs.lib.noaa.gov/rescue/dwm/data_rescue_daily_weather_maps.html. Nine cold fronts passed the Northeast during July 1 - August 15, 2004, with only 2005 exceeding this number. Conversely, only five fronts passed Boston during July 2000. Results for the Southeast are even more impressive (Table 1), with more frontal passages (seven) than during any of the other years. Surface analyses for five of the strongest frontal systems over the Southeast are shown in Figure 5 (July 20-Flight 10, July 25-Flight 12,

August 2-Flight 15, August 6-Flight 16, and August 15-Flight 19). In most of these cases, the cold front already had passed the Northeast and now stretched into the deep South, sometimes reaching the Gulf Coast and even central Florida. Well developed high pressure centers were located behind each front. These fronts typically were preceded by widespread deep convection, and each brought somewhat cooler, drier air to the Southeast, replacing the hot, humid conditions that are typical of summer. Each of the frontal cases was associated with a well developed trough aloft that provided the necessary upper- level support for the surface fronts to extend so far south (examples are in Figure 2).

The INTEX flight planning team hoped to sample a stagnant high pressure region over the Northeast. Such stagnant conditions would facilitate the buildup of pollution from the major urban areas which then would be swept northeastward by the next cold front where it could be further sampled by successive INTEX flights over the western Atlantic Ocean. Unfortunately, such stagnant conditions did not occur during the mission. Instead, the frequent cold frontal passages during 2004 (Table 1) indicate an active summer period, with an average of only 4.6 days between successive cold frontal passages. Only the corresponding period during 2005 had a shorter span between fronts.

The contiguous U.S. experienced its 16th coolest summer on record and seventh coolest August [*NOAA*, 2004, http://www.noaanews.noaa.gov/stories2004/s2319.htm]. Minnesota had its coldest August on record, while six consecutive daily record minima were established at Meridian, MS and Mobile, AL. This was their longest summer cold spell in their observed weather history dating back to the mid 1800's. Conversely, only three western states averaged much warmer than the long term mean (years 1895-2003).

The colder than normal conditions over most of the country did not occur continuously, but mostly were due to several powerful cold outbreaks such as between July 26-30 and August 10-16 during the INTEX period [*Pennsylvania State University*, 2004, http://pasc.met.psu.edu/PA_Climatologist/highlight20041214/summer_2004.html]. Summer 2004 was associated with weak El Nino conditions as sea surface temperatures increased over much of the central and east-central equatorial Pacific [*NOAA*, 2006, http://www.cdc.noaa.gov/people/klaus.wolter/MEI].

4.2 Alaskan Wildfires

Wildfires over portions of Alaska and western Canada are a common occurrence during the warm season. However, fire activity during the INTEX-NA 2004 period reached record breaking proportions. Forest fire emissions not only affect the local surroundings, but also influence the atmosphere on regional scales [*Tanimoto et al.*, 2000; *Kato et al.*, 2002], continental scales [*Wotawa and Trainer*, 2000], and even hemispheric scales [*Forster et al.*, 2001; *Wotawa et al.*, 2001; *Damoah et al.*, 2004; *Spichtinger et al.*, 2004; *Yurganov et al.*, 2004; *Novelli et al.*, 2003]. Air quality in the United States is affected by wildfires in Canada [*Wotawa and Trainer*, 2000; *McKeen et al.*, 2002; *DeBell et al.*, 2004] and Siberia [*Jaffe et al.*, 2004]. The INTEX and ICARTT aircraft sampled the Alaskan and Canadian plumes far downwind of their sources on numerous occasions.

Excellent discussions of the 2004 Alaskan fires are provided by *Richmond and Shy* [2005] and *Damoah et al.* [2005]. May 2004 was a wet period for most of Alaska, and few fires occurred. Conditions then changed dramatically. Alaska during the second half of June was very warm and dry, with some areas breaking all time maximum

235 temperatures (see http://climate.gi.alaska.edu) and recording only 25-50% of normal
236 precipitation, the third driest summer on record [*Rozell*, 2004]. The fires that began
237 during this period grew explosively, fanned by surface winds of ~ 32 km h^{-1} [*Rozell*,
238 2004]. The fires created dense smoke over nearby areas. Temperatures during July were
239 only slightly above normal, but there were many thunderstorms producing record
240 amounts of lightning. Fires in northwestern Canada began in mid July, i.e., later than
241 those in Alaska. Figure 6a shows MODIS imagery of fire locations in Alaska on July 1
242 and (panel b) near the border of Saskatchewan and Manitoba on July 15. The
243 widespread dense plumes of smoke are clearly visible. August also was a month of above
244 normal temperatures and below normal precipitation, causing the fires to continue raging.
245 The meteorological patterns described earlier provided optimum conditions for the
246 record breaking wildfire activity. Specifically, the strong high pressure ridge that
247 developed over Alaska during the second half of June persisted several months (Figure
248 1). The mission averaged height anomaly at 500 hPa was ~ 70 m. Unlike typical
249 summers, the persistent ridge prevented transient eastward moving low pressure systems
250 from entering the state. These systems would have brought cooler temperature and
251 widespread rainfall. Instead, a warm and often unstable air mass blanketed the area,
252 producing thunderstorms with widespread, often intense lightning on some days. For
253 example, on 15 July, 9,022 cloud-to-ground flashes were detected over the state by the
254 Alaskan lightning detection network. This was the greatest 24 hour total since the
255 network became operational 25 years earlier. Unfortunately, these storms did not produce
256 sufficient rainfall to douse the existing fires, but instead their lightning started new fires.

257 By the end of the year, the 707 fires in Alaska alone had burned 2.7 x 10^6 ha,
258 which is 8 times the 10-year average [U.S. National Interagency Fire Center
259 (http://www.cidi.org/wildfire)], surpassing the old record of 2 x 10^6 ha during 1957
260 [*Damoah et al*., 2005]. In western Canada, wildfires also were much greater than the 10-
261 year average (Canadian Interagency Forest Fire Center). The total emission of CO due to
262 fires in North America during 2004 has been estimated at 27 Tg [*Turquety et al.,* 2006]
263 based on burning inventory techniques. This total came from two major burning areas:
264 Alaska-Yukon (21 Tg) and north-central Canada (6 Tg). *Pfister et al*. [2005] obtained the
265 value 30 ± 5 Tg based on inverse modeling of MOPITT CO observations. These record
266 breaking emissions represent a major perturbation to typical summertime conditions.
267 The atmospheric flow patterns that created conditions conducive to the record-
268 breaking fires also transported their burning by-products far downwind and into the
269 INTEX and ICARTT domains. Specifically, persistent high pressure ridging over Alaska
270 and the West Coast, together with frequent troughs over the East Coast (Figures 1-2),
271 often carried the burning by-products eastward or southeastward. These plumes were
272 sampled by the INTEX DC-8 on numerous flights. For example, Figure 7a shows the
273 smoke plume over the Labrador Sea off the coast of Newfoundland on July 19. Figure 8
274 shows backward trajectories along three segments of Flight 9 in this area on July 18, one
275 day earlier than the image, but still containing the major smoke plume. These trajectories,
276 arriving at the DC-8 at altitudes ranging from 500 to 300 hPa, clearly show long range
277 transport from the fire regions. In this example the DC-8 sampled air that had originated
278 over the burning areas four to ten days earlier, depending on aircraft altitude and
279 meteorological conditions. The burning by-products also traversed several different

routes. Figure 6b shows a large smoke plume over the Gulf Coast, also on July 19. Backward trajectories (not shown) reveal that the smoke over Arkansas, Louisiana, southeastern Texas, and coastal Mississippi had traveled eastward over Canada and then southward along the Mississippi River—a distance of several thousand kilometers. This type of southward extension was sampled by the DC-8 during several INTEX flights (not shown). For example, *Morris et al*. [2006] showed that Alaskan and Canadian forest fires exacerbated ozone pollution over Houston, Texas, on July19-20, 2004.

The smoke plumes from Alaska and western Canada were clearly visible to those onboard the DC-8. For example, Figure 9 contains two pictures taken by the lead author from the cockpit of the DC-8 as it approached Portsmouth, NH on July 20 (Flight 10). The aircraft's altitude at the time was approximately 600 hPa (~14,000 ft). In panel a) the plume is highlighted against cumulus clouds in the background. Careful inspection reveals one thick, dense pollution layer, as well as several thinner, weaker layers. Shortly after the first photo was taken, the plume terminated (panel b) just before the DC-8 landed in Portsmouth. Backward trajectories from the area of the smoke plume in Figure 9 are shown in Figure 10. The polluted air observed and sampled by the DC-8 originated over regions of fire activity in Alaska 6 -7 days earlier.

The long range transport of smoke observed during INTEX-NA is consistent with recent studies showing that burning by-products are not merely emitted in the boundary layer but also at much higher altitudes where horizontal winds are stronger [*Fromm et al*., 2000, 2005; *Fromm and Servramclx*. 2003]. Using a chemical transport model, *Colarco et al*. [2004] showed that an injection height of 2-6 km produced the best agreements with observed conditions for Canadian wildfires during July 2002. *Pfister et al*. [2005]

303 distributed the 2004 emissions uniformly up to height of 400 mb to achieve best
304 agreement with a chemical transport model.

305 Deep convection that is triggered or enhanced by forest fires (pyro-convection) can
306 even deposit burning by-products in the upper troposphere and lower stratosphere
307 [*Fromm et al.,* 2003, 2005; *Livesey et al*., 2004; *Immler et al.*, 2005; *Jost et al*., 2004].
308 *Andreae et al*. [2004] proposed that burning-derived aerosols can affect cloud
309 microphysics such that latent heating at high altitudes is enhanced, thereby increasing the
310 height of a storm.

311 *Damoah et al.* [2006] showed that strong pyro-convective events occurred during
312 the Alaskan and Canadian wildfires of 2004. In some cases, convective cloud tops as cold
313 as -60^{o}C were almost coincident with major fire regions. That convection penetrated the
314 lower stratosphere, reaching 3 km above the tropopause. The downstream INTEX and
315 ICARTT data show evidence of these byproducts as high as 10 km [*de Gouw et al*., 2006;
316 *Kittaka et al.*, 2006]. As a result of the high altitude CO observations, *Turquety et al*.'s
317 [2006] chemical transport modeling of 2004 Alaskan wildfires distributed emissions as
318 40% in the boundary layer, 30% in the middle troposphere, and 30% in the upper
319 troposphere. This distribution provided the best agreement with CO measurements from
320 the MOPITT space-borne instrument [*Deeter et al.* 2003].

321 Papers in this special INTEX section that investigate wildfire emissions include
322 *Clarke et al.* [2006] and *Kittakai et al*. [2006].

323

324 **4.3 Quasi-Lagrangian Flights**

325 One of the goals of ICARRT was for the European aircraft to sample air over the
326 eastern Atlantic Ocean that had been sampled previously by the INTEX DC-8 over the

United States or the western Atlantic Ocean. This multiple sampling would permit the evolution of plume chemistry to be studied. By using a combination of backward and forward trajectories together with chemical transport models, the flight planning teams each day considered whether this scenario was occurring. Since it was unlikely that the European aircraft would sample the identical parcels sampled earlier, this approach was denoted "quasi"- Lagrangian, instead of truly Lagrangian. The INTEX and ICARTT aircraft conducted several "wing tip to wing tip" inter-comparison flights to insure that the data from each aircraft could be used in the quasi-Lagrangian experiments. Photographs during the inter-comparison flights show that the pilots went to great lengths to provide minimal aircraft separation (Figure 11).

Results indicate that the quasi-Lagrangian objective was met to varying degrees during a number of flights. Specifically, air sampled by the DC-8 on July 6, 8, 10, 12, 15, 18, 25, 28, and August 14 appeared to be transported to Europe and beyond. For example, Figure 12 shows 10 day forward trajectories from the same three flight segments shown earlier in Figure 8. Depending on the synoptic situation, the burning plumes crossed the Atlantic Ocean in as little as three days, reaching England, the Mediterranean Sea, and later Asia. Many of the parcels remained at approximately the same altitude at which they were sampled by the DC-8; however, some experienced considerable subsidence, especially those on leg 26 as they passed east of a high pressure region. One also should note that some trajectories extend into the Arctic regions, contributing to Arctic haze [*Stohl*, 2006]. It is clear that major pollution from any one location on the Earth truly is transported on a global scale.

351

352 **4.4 Precipitation and lightning**

353 Precipitation is an important factor in atmospheric chemistry. For example,
354 scavenging of soluble species by precipitation can deplete their concentrations (e.g.,
355 *Cohan et al*. [1999], *O'Sullivan et al.* [1999]). Furthermore, precipitation is due to rising
356 motion that can transport species to higher altitudes. Precipitation in the middle latitudes
357 often is due to well developed low pressure centers and their associated frontal systems
358 (e.g., those in Figures 2 and 5). However, smaller scale forcing such as the sea breeze
359 and topography also are important.

360 Lightning generally is confined to deep convective clouds that contain strong
361 updrafts and have ice in their upper reaches. Thus, clouds producing lightning are
362 expected to be important mechanisms by which surface-based chemical species are
363 rapidly transported to higher altitudes where they can be quickly carried horizontally to
364 distant locations by the relatively strong upper tropospheric winds. Furthermore,
365 lightning is a source of nitrogen oxides in the atmosphere [e.g., *Ehhalt et al*., 1992;
366 *Lawrence et al*., 1994; *Bond et al*., 2001].

367 Figure 13 shows the horizontal distribution of cloud-to-ground lightning during
368 the composite 6 week INTEX period, where the flashes have been counted over boxes
369 that are 0.1^{o} latitude (11 km) on each side. Florida and the eastern Gulf Coast experience
370 the greatest lightning during INTEX, with large areas exceeding 500 flashes per 11 km
371 square box. This lightning is due to cold fronts that atypically reached this far south
372 (Section 3.1) and due to sea breeze circulations (e.g., *Lericos et al*., 2002; *Smith et al*.,
373 2005), afternoon heating, and other small scale forcing mechanisms. The Great Plains
374 and Mississippi and Ohio River Valleys also experience abundant CG lightning that often

375 was due to passing transient synoptic systems. Conversely, there is much less lightning
376 over the West Coast, Pacific Northwest, and New England. The INTEX-NA lightning
377 pattern has many similarities to the mean annual flash densities calculated by *Orville and*
378 *Huffines* [2001] during the 1989-1998 period. Thus, INTEX lightning distributions
379 appear representative of climatology.

380 Historical CG lightning counts are presented in Table 2 for a rectangle enclosing
381 the contiguous U.S. and the area just north of the Great Lakes (66^{o}W-126^{o}W, 25^{o}N-
382 50^{o}N). The NLDN underwent a major upgrade during 2002, yielding an improved
383 detection efficiency and location accuracy [*Cummins et al.,* 2006]. These earlier data are
384 not considered here since the resulting flash counts would be inconsistent with the more
385 recent results. July 2004, with 7,691,566 flashes, had the greatest number of the three
386 year period. Conversely, August 1-15, 2004 had the smallest total of the three years.
387 Although the overall INTEX period, with 10,692,608 CG flashes, had the smallest flash
388 count of the most recent three years, the difference is not great. Thus, 2004 appears
389 typical of at least the most recent years. It is important to note that there are
390 approximately two cloud discharges for every cloud to ground flash [*Boccippio et al*.,
391 2001; *Bond et al.,* 2001]. Thus, the total number of CG, intercloud and intracloud flashes
392 likely exceeds 33 million during INTEX-NA. *Bond et al*. [2001] assumed an NO
393 production rate of 6.7×10^{26} molecules for each CG flash and 6.7×10^{25} molecules for
394 each cloud flash. They found that CG flashes produced more NO_x than cloud flashes, in
395 spite of the much smaller number of CG flashes. *Bond et al*. [2001] concluded that
396 regional emissions of NO_x by lightning can be significant during the summertime and

397 may play a major role in ozone formation in the free troposphere. Current data certainly
398 suggest that lightning was a major producer of NO_x during INTEX-NA.

399 Figure 14 contains CG flash counts for each INTEX day in the area described
400 above. The first half of July was the most lightning prolific period, with much of the
401 lightning occurring east of the Mississippi River (not shown). This major lightning
402 activity occurred during a period of relatively zonal flow (Figures 2 and 4). The second
403 half of July and first half of August contained much less lightning, although there were
404 several periods of intense activity that corresponded to the southward extending cold
405 fronts and major sea breeze activity.

406 The DC-8 flew near active deep convection on several missions (e.g., Figure 15
407 taken on July 20 over the southeast U.S.) and detected convective chemical signatures on
408 many other flights. DC-8 Flights 7 and 12 on July 12 and 25, respectively, are good
409 examples of when intense convection was sampled both during and prior to the flight.
410 July 12 was the third most active lightning day during INTEX-NA (Figure 14), occurring
411 during the general period of greatest flash activity. The DC-8's track over the Southeast
412 and Midwest is superimposed on a GOES infrared image approximately half way through
413 the flight in Figure 16a. The bright white areas along the southern Appalachians, Gulf
414 Coast, and northern Great Plains represent areas of deep convection that produced intense
415 lightning. DC-8 flight 12 (Figure 16b) sampled recent lightning over the Appalachians.
416 This flight occurred during a secondary peak in flash counts (Figure 14).

417 We determined which DC-8 legs sampled air that likely exhibited a lightning
418 influence. Our procedure was to calculate backward trajectories at 1 min intervals along
419 each DC-8 flight leg. Using the trajectory methodology described in Section 2, each

trajectory's first encounter with nearby CG lightning was determined. A trajectory was considered to be lightning "influenced" if at a given time along its history there was at least one NLDN-detected CG flash within a 1.0 deg radius of the trajectory's location and within a 1 h temporal window. This procedure is similar to that used by *Jeker et al*. [2000].

Figure 17a contains averaged streamlines from July 8 – 12 at 500 hPa, the DC-8 Flight 7 track, as well as lightning color coded by age for the four day period ending on July 12 (the flight day). Flight 7 sampled air with a recent lightning influence (e.g., within 12 h of sampling) due to storms over the Dakotas, Missouri, eastern Tennessee, and eastern Georgia. More aged convective and lightning influences also were detected from storms on previous days over the Midwest, Gulf Coast, and Gulf of Mexico. Similarly, Flight 12 (Figure 17b) sampled recently lightning influenced air from storms over the spine of the Appalachians (< 6 h). Slightly older samples were from lightning over Georgia, and the lower Mississippi River Valley. Finally, lightning influenced air was sampled from much older storms (3-4 days prior) over the Midwest and northeastern states. These two flights clearly indicate that the DC-8 sampled lightning influenced air with a wide range of ages and lofted from a variety of geographical origins (e.g., lofted over cities, forests, etc).. INTEX-NA papers providing detailed discussions of precipitation, convective, and lightning chemical signatures include *Bertram et al*. [2006], *Bűker et al*. [2006], *Fried et al*. [2006], and *Garrett et al*. [2006].

5.0 Summary Data

It is informative to consider the past histories of parcels sampled by the DC-8 during the eighteen science flights of INTEX-NA. Browell et al. [2006] used data from

444 the Differential Absorption Lidar (DIAL) instrument to perform large-scale air mass
445 characterizations during INTEX. We have used a different approach, calculating
446 backward trajectories at 1 min intervals along each DC-8 flight leg. Our trajectory
447 methodology was described in Section 2, and the complete trajectory dataset is available
448 at http://www-air.larc.nasa.gov/cgi-bin/arcstat, with images available at
449 http://fuelberg.met.fsu.edu/research/intexa. Hourly positions of all 9,409 DC-8
450 trajectories were compared with fields from the GFS model which has 6 h temporal and
451 0.5 deg spatial resolution. At each hour back along the trajectory, its height was checked
452 against the model data at the closest grid point. The first encounter with several types of
453 environments was recorded (Table 3).

454 Convective influence was assumed if the grid point nearest the trajectory had
455 grid-scale convective precipitation during the previous hour and the trajectory passed
456 below the level of the highest cloud tops. If no high clouds were reported, convective
457 influence was assumed if the trajectory encountered convective precipitation and was
458 below 500 hPa. To determine boundary layer encounters, each trajectory's pressure was
459 compared to the closest model-derived PBL height. A residual layer encounter was
460 reported if the trajectory passed above the PBL, but below the level of the previous day's
461 boundary layer. Finally, stratospheric encounters were located by comparing the
462 trajectory's pressure with the model reported tropopause height.

463 A trajectory's first encounter with nearby lightning also was determined. A
464 trajectory was considered to be lightning "influenced" if there was at least one NLDN-
465 detected CG flash within 0.5 deg. (or 1.5 deg) latitude/longitude and within 30 min of its
466 position. Another set of statistics was compiled for trajectories encountering 60 or more

467 flashes within these same spatial and temporal limits. As noted earlier, the NLDN only
468 detects CG flashes, and only a fraction of the total flashes are CG.

469 Results of the encounter procedure are quite interesting (Table 3). Only 8.3% of
470 the DC-8's trajectories did not encounter GFS-derived convection during the 10 day run
471 period. Many of these convective encounters occurred during the first day, e.g., 21.4%
472 during the first 6 h and 46.4% during the first 24 h. The percentages are less than 6.5% at
473 all later periods. These results indicate that many of the DC-8 samples will exhibit a
474 convective influence of varying age. Almost half of the DC-8's trajectories encountered
475 the PBL and the residual layer during the 10 day runs, with many of these encounters
476 occurring during low level flight legs. One should note that our procedure does not
477 consider small scale processes such as turbulence that are not handled adequately by the
478 GFS model. Nonetheless, pollutants lofted from near the surface by processes that were
479 resolvable by the GFS model were sampled frequently by the DC-8 during INTEX.

480 The DC-8 did not often sample "pure" stratospheric air (i.e., air above the
481 tropopause) (Table 4). Only 27.3% of the trajectories exceeded the tropopause height
482 during the entire 10 day period. However, our simple diagnostic approach does not
483 consider stratospheric air that has been mixed into the lower levels by turbulence
484 associated with tropopause folding, the jet stream, or other mechanisms. In-flight
485 discussions suggested numerous occasions when the samples appeared to have a
486 stratospheric component. *Tarasick et al.* [2006] and *Thompson et al*. [2006], both in this
487 special section, discuss stratospheric contributions to INTEX-NA observations. Finally,
488 one should note that most of the DC-8 trajectories passed over land during the previous
489 10 days, i.e., only 6.5% remained over water during the entire period. Approximately

490 70% of the parcels either were sampled over land or encountered land within 6 h of
491 sampling. Thus, the INTEX-NA chemical data are heavily influenced by land-based
492 processes where the radiation profiles are different and there are distinct emissions and
493 chemical processes.

494 We compared our back trajectory encounters based on GFS-derived convection
495 against the likelihood of convective encounters by chance (Table 4). The GFS data
496 revealed that 12.5% of the grid points contained convection when the entire INTEX-A
497 campaign is considered. Therefore, we assumed a 12.5% random chance of encountering
498 convection every 6 h and calculated binomial probabilities [*Wilks*, 2006] to determine the
499 chance of at least 1 convective encounter over the time window. This is a simplistic
500 approach that, for example, does not consider the diurnally varying nature of deep
501 convection or its tendency to be associated with certain synoptic scale or mesoscale
502 systems (e.g., fronts, sea breezes, etc.). Nonetheless, the major finding is that the DC-8
503 sampled convective outflow considerably more often during the first 6 h than expected
504 based on chance alone (21.4% vs. 12.5%). This is consistent with our common flight
505 planning objective of being near or downwind of active convection or other
506 meteorologically interesting features.

507 Convection as defined by the GFS model could be erroneously placed, and it does
508 not indicate the presence of lightning. Therefore, we computed encounters with NLDN-
509 derived CG lightning. Table 3 shows that results depend greatly on how close the DC-8's
510 trajectory must be to the flash to be considered an encounter (within 0.5 or 1.5 deg), and
511 on the number of flashes that must be contained within that search region (1 or 60
512 flashes). Considering the uncertainties in the trajectories, and that only CG flashes (not

513 total flashes) were considered, the discussion below focuses on the category of one
514 NLDN flash within 1.5 deg of the trajectory location. It should be noted that this is the
515 most generous criteria considered for assessing lightning influence.

516 The DC-8 encountered lightning (as defined above) considerably less often than it
517 encountered GFS-derived convection (Table 3). 32.9% of the trajectories did not
518 encounter any lightning of this type during their 10 day periods. Conversely, 42.1% of
519 the trajectories encountered lightning within 24 h, and there were 56.7% encounters
520 during the first 48 h. These statistics confirm that the DC-8 often flew near active deep
521 convection, and that lightning induced NO_x likely is an important constituent of the
522 INTEX samples, as described by *Bertram et al*. [2006] during INTEX-NA and proposed
523 by *Bond et al.* [2001] in a climatological study.

524 **6. Conclusions**

525 This paper has described meteorological conditions during the Intercontinental
526 Chemical Transport Experiment—North America (INTEX-NA) which was conducted
527 over the contiguous United States and adjacent areas during July and August 2004.
528 Anomalously strong and persistent high pressure dominated Alaska and western Canada
529 during much of the INTEX-NA period. This blocking pattern prevented low pressure
530 areas over the North Pacific from bringing cooler temperatures and abundant
531 precipitation to Alaska. The result was unusually hot and dry conditions over much of the
532 area. Relatively zonal flow dominated the contiguous U.S. during the first two weeks of
533 the mission, while a series of large amplitude troughs traversed the eastern half of the
534 country during the final four weeks. Several of these troughs extended the full north to
535 south length of the eastern U.S., reaching over the Gulf of Mexico.

536 The unusually strong middle tropospheric troughs were accompanied by a series
537 of cold fronts that also reached as far south as the Gulf of Mexico. Fronts extending this
538 far south during the summer are uncommon. During the INTEX-NA period, seven cold
539 fronts passed Atlanta, GA, the greatest number during the period 2000-2005. These
540 fronts brought record low temperatures to portions of the Great Plains and South. Frontal
541 passages over the Northeast were only somewhat above average, but the short average
542 time interval between passages (4.6 days) meant that stagnant high pressure centers
543 containing abundant pollution never formed over the area

544 The persistent high pressure over Alaska provided ideal conditions for wildfires in
545 Alaska and western Canada. As a result, a record number of acres was burned during
546 Summer 2004, surpassing the old record established in 1957. The location of the
547 persistent ridge also meant that burning by-products often were transported
548 southeastward toward the contiguous U.S. and the INTEX domain. These plumes were
549 sampled by the DC-8 during numerous flights. During some flights, forward trajectories
550 and satellite imagery showed that the plumes later were carried to parts of Europe, Africa,
551 and even the Arctic. In some cases the transported pollution near Europe was sampled in
552 a quasi-Lagrangian sense by INTEX's international partners participating in the ICARTT
553 experiment. It is clear that the atmospheric chemistry during INTEX-NA was heavily
554 influenced by the record breaking fires and the long range transport of their by-products.

555 Cloud to ground (CG) lightning data showed that horizontal patterns and numbers
556 of lightning flashes during INTEX-NA were similar to those 2003 and 2005. Statistics
557 derived from 10 day backward trajectories indicated that the DC-8 sampled lightning
558 influenced air ~ 65% of the time. If convection derived from the GFS meteorological

559 model is considered, the DC-8 sampled convectively influenced air ~92% of the time,
560 with many of these encounters occurring within 6 h of in situ sampling. It is clear that
561 deep convection and lightning were important factors during INTEX-NA.

562 In conclusion, INTEX-NA was a period of active weather. The period exhibited
563 several meteorologically anomalous aspects that should be considered when comparing
564 its chemical measurements with those from other periods.

565 **Acknowledgments.** This research was sponsored by NASA's Tropospheric
566 Chemistry Program under Grants NNG04GC33G and NNG06B43G to Florida State
567 University. Satellite imagery was provided by David Westberg of Science Applications
568 International Corporation (SAIC) working at NASA Langley Research Center. Jeremy
569 Halland at Florida State assisted in preparing the manuscript. The NLDN lightning data
570 were provided courtesy of Marshall Space Flight Center using data obtained from Vaisala
571 Inc. Finally, we appreciate the helpfulness of the DC-8 crews and support staff during the
572 INTEX-A preparation and deployment periods that allowed us to satisfy our science
573 objectives.

REFERENCES

Andreae, M.O. D. Rosenfeld, P. Artaxo, A.A. Costa, G.P. Frank, K.M. Longo, and M.A.F. Dias, Smoking rain clouds over the Amazon, *Science*, 303, 1337-1342, 2004.

Bertram, T.H., A. Perring, P. Wooldridge, R. Cohen, J. Dibb, E. Scheuer, J. Crounse, P. Wennberg, S. Vay, S. Kim, G. Huey, J. Walega, A. Fried, M. Porter, H. Fuelberg, B. Heikes, G. Sachse, M. Avery, and A. Clarke, Convection and the age of air in the upper troposphere, Submitted to *J. Geophys. Res.*, 2006.

Blake, N.J., D.R. Blake, I. Simpson, J. Lopez, N. Ciskowski. A. Swanson, A. Kazenstein, S. Meinardi, B. Sive, J. Colman, E. Atlas, F. Flocke, S. Vay, M. Avery, and F.S. Rowland, Large scale latitudinal distribution of NMHCs and selected halocarbons in the troposphere over the Pacific Ocean during the March-April 1999 Pacific Exploratory Expedition (PEM-Tropics B), *J. Geophys. Res*., *106*, 32627-32644, 2001.

Boccippio, D. J., K. L. Cummins, H. J. Christian, S. J. Goodman, Combined Satellite- and Surface-Based Estimation of the Intracloud Cloud-to-Ground Lightning Ratio over the Continental United States. *Mon. Wea. Rev.*, 129, 108-122, 2001.

Bond, D.W., R. Zhang, X. Tie, G. Brasseur, G. Huffines, R.E. Orville, and D.J. Boccippio, NOx production by lightning over the continental United States, *J. Geophys. Res*., 106, 27701-27710, 2001.

Browell, E.V., M.A. Fenn, J.W. Hair, C.F. Butler, A. Notari, S.A. Kiio, S. Ismail, M.A.

Avery, R.B. Pierce, and H.E. Fuelberg, Large-scale air mass characteristics observed during the summer over North America and western Atlantic Ocean, *J. Geophys. Res*., 2006.

Bűker, M. Hitchman, R.B. Pierce, E.V. Browell, Kis, and G. Tripoli, Convective initiation of long-range stratospheric influence during INTEX-NA: Local ozone flux values, *J. Geophys. Res*., 2006.

Clarke, A.D., V. Kapustin, S.G. Howell, C.S. McNaughton, Y Shinozuka, B. Anderson, and J. Dibb, Aerosol from biomass burning and regional pollution over North America during INTEX-NA: Humidity response and the wavelength dependence of scattering and absorption, *J. Geophys. Res*., 2006.

Cohan, D.S., M.G. Schultz, and D.J. Jacob, Convective injection and photochemical decay of peroxides in the tropical upper troposphere: Methyl iodide as a tracer of marine convection, *J. Geophys. Res*., *104*, 5717-5724, 1999.

Colarco, P.R., M.R. Schoeberl, B.G. Doddridge, L.T. Marufu, O. Torres, and E.J. Welton, Transport of smoke from Canadian forest fires to the surface near Washington, D.C.: Injection height, entrainment, and optical properties, *J. Geophys. Res*., 109, doi:10.1029/2003JD004248, 2004.

Cummins, K. L., J.A. Cramer. C.J. Biagi, E.P. Krider, J. Jerauld, M.A. Uman, and V.A. Rakov, The U.S. national lightning detection network: Post-upgrade status, 2nd Conf. Meteor. Applications of Lightning Data, Amer. Meteor. Soc., Atlanta, paper 6.1, 2006.

Cummins, K. L., M. J. Murphy, E. A. Bardo, W.L. Hiscox, R. B. Pyle, and A. E. Pifer, A combined TOA/MDF technology upgrade of the U.S. National

Lightning Detection Network. *J. Geophys. Res*., **103**, 9035-9044, 1998.

Damoah, R., N. Spichtinger, C. Forster, P. James. I. Mattis, U. Wandinger, S. Beirle, T. Wagner, and A. Stohl, Around the world in 17 days—hemispheric-scale transport of forest fire smoke from Russia in May 2003, *Atmos. Chem. Phys*., 4, 1311-1321, 2004.

Damoah, R., N. Spichtinger, R. Servranckx, M. Fromm, E.W. Eloranta, I.A. Razenkov, P. James, M. Shulsi, C. Forster, and A. Stohl, Transport modeling of a pyro-convection event in Alaska, *Atmos. Chem. Phys. Discuss*., 5, 6185-6214, 2005.

Damoah, R., N. Spichtinger, R. Servranckx, M. Fromm, E.W. Eloranta, I.A. Razenkov, P. James, M. Shulsi, C. Forster, and A. Stohl, A case study of pyro-convection using transport model and remote sensing data, *Atmos. Chem. Phys*., 6, 173-185, 2006.

DeBell, L.J., R.W. Talbot, J.E. Dibb, J.W. Munger, E.V. Fischer, and S.E. Frolking, A major regional air pollution event in the northeastern United States caused by extensive forest fires in Quebec, Canada, *J. Geophys. Res*., 109, doi:10.1029/2004JD004840, 2004.

Deeter, M.N., et al., Operational carbon monoxide retrieval algorithm and selected results for the MOPITT instrument, *J. Geophys. Res*., 108, doi:10.1029/2002JD003186, 2003.

De Gouw, J.A., C. Warneke, A. Stohl, A.G. Wollny, C.A. Brock, O.R. Cooper, J.S. Holloway, M. Trainer, F.C. Fensenfeld, E.L. Atlas, S.G. Donnelly, V. Stroud, and A. Lueb, The VOC composition of merged and aged forest fire plumes from Alaska and Western Canada, in press, *J. Geophys. Res*., 2006.

Ehhalt, D.W., F. Roher, and A. Wahner, Sources and distributions of NO_x in the upper

troposphere at northern midlatitudes, *J. Geophys. Res., 97*, 9781-9793, 1992.

Fehenseld, F.C., et al., International Consortium for Atmospheric Research on Transport and Transformation (ICARTT): North America to Europe: Overview of the 2004 summer field study, *J. Geophys. Res*., 2006.

Forster, C., U. Wandinger, G. Wotawa, P. James, I. Mattis, D.Althausen, P. Simmonds, S. O'Doherty, S. Jennings, C. Kleefeld, J. Schnieder, T. Trickl, S.Kreipl, H. Jäger, and A. Stohl, Transport of boreal forest fire emissions from Canada to Europe, *J. Geophys. Res*., 106, 22817-22906, 2001.

Fried, A., J. Walega, J. Olson, J. Crawford, G. Chen, B. Heikes, D. O'Sullivan, and H. Shen, The role of convection in redistributing formaldehyde to the upper troposphere over North America and the North Atlantic during the summer 2004 INTEX campaign, *J. Geophys. Res*., 2006.

Fromm, M., J. Alfred, K. Hoppel, J. Hornstein, R. Bevilacqua, E. Shettle, R. Servranckx, Z. Li, and B. Stocks, Observations of boreal forest fire smoke in the stratosphere by POAM III, SAGE II, and lidar in 1998, *Geophys. Res. Lett*., 27, 1407-1410, 2000.

Fromm, M.D. and R. Servranckx, Transport of forest fire smoke above the tropopause by supercell convection, *Geophys. Res. Lett*., 30, 1542, doi:10.1029/2002GL016820, 2003.

Fromm, M., R. Bevilacqua, R. Servranckx, J. Rosen, P.J. Thayer, J. Herman, and D. Larko, Pyro-cumulonimbus injection of smoke to the stratosphere: Observations and impact of a super blowup in northwestern Canada on 3-4 August 1998, *J. Geophys. Res*., 110, doi:.1029/2004JD005350, 2005.

Fuelberg, H.E., R.O. Loring, Jr., M.V. Watson, M.C. Sinha, K.E. Pickering, A.M. Thompson, G.W. Sachse, D.R. Blake, and M.R. Schoeberl, TRACE-A Trajectory intercomparison 2. Isentropic and kinematic methods, *J. Geophys. Res., 101*, 23927-23939, 1996.

Fuelberg, H.E., R.E. Newell, S.P. Longmore, W. Zhu, D.J. Westberg, E.V. Browell, D.R. Blake, G.L. Gregory, and G.W. Sachse, A meteorological overview of the PEM-Tropics period, *J. Geophys. Res*., *104*, 5585-5622, 1999.

Fuelberg, H.E., J.R. Hannan, P.F.J. van Velthoven, E.V.Browell, G. Bieberbach, Jr., R.D. Knabb, G.L. Gregory, K.E. Pickering, and H.B. Selkirk, A meteorological overview of the SONEX period. *J. Geophys. Res., 105*, 3633-3651, 2000.

Fuelberg, H. E., C. M. Kiley, J. R. Hannan, D. J. Westberg, M. A. Avery, R. E. Newell, Atmospheric transport during the TRAnsport and Chemical Evolution over the Pacific TRACE-P experiment, J. Geophys. Res., 108(D20), 8782, doi:10.1029/2002JD003092, 2003.

Garrett, T.J., L. Avey, P. Palmer, C. Brock, T. Ryerson, A. Neuman, and J. Holloway, Observational quantification of precipitation scavenging of anthropogenic HNO_3 and CCN during ICARTT, *J. Geophys. Res*., 2006.

Immler, F., D. Engelbart, and O. Schrems, Fluorescence from atmospheric aerosol detected by a lidar indicates biogenic particles in the stratosphere, *Atmos. Chem. Phys*., 5, 345-355, 2005.

Jaffe, D., I Bertschi, L. Jaegle, P. Novelli, J.S. Reid, H. Tanimoto, R. Vingarzan, and D.L. Westphal, Long-range transport of Siberian biomass burning emissions and

impact on surface ozone in western North America, *Geophys. Res. Lett.*, 31, doi:10.1029/2004GL020093, 2004.

Jeker, D.P., L. Pfister, A.M. Thompson, D. Brunner, D.J. Boccippio, K.E. Pickering., Heini Wernli, Y. Kondo, and J. Staehelin*, J. Geophys. Res*., 105, 3679-3700, 2000.

Jost, H.J., K. Drdla, A. Stohl, L. Pfister, M. Loewenstein, J.P. Lopez, P.K., Hudson, D.M. Murply, D.J. Cziczo, M. Fromm, T.P. Bui, J., Dean-Day, C. Gerbig, M.J. Mahoney, E.C. Richard, N. Spichtinger, E.M. Weinstock, J.C. Wilson, and I. Xueref, In situ observations of mid-latitude forest fire plumes deep in the stratosphere, *Geophys. Res. Lett*., 31, 11101, doi:10.1029/2003GL019253, 2004.

Kalnay, E., *et al.*, The NCEP/NCAR reanalysis 40-year project, *Bull. Am. Meteorol. Soc*., 77, 437-471, 1996.

Kato, S., P. Pochanart, J. Hirokawa, Y. Kajii, H. Akimoto, Y. Ozaki, K. Obi, T. Katsuno,D.G. Streets, and N.P. Minko, The influence of Siberian forest fires on carbon monoxide concentrations at Happo, Japan, *Atmos. Environ*., 36, 385-390, 2002.

Kittakai, C., B. Pierce, J. Szykman, J. Al-Saadi, T. Schaack, G. Tripoli, A. Chu, M. Avery, D. Fairlie, and E. Browell, An aerosol model study with MODIS AOD assimilation: Assessing impacts of Alaskan smoke on the continental U.S. air quality during ICARTT/INTEX-NA, *J. Geophys. Res*., 2006.

Lawrence, M.G., *et al*., *Handbook of Atmospheric Electrodynamics*, Lightning and atmospheric chemistry: The rate of NO_x production in 1994, Radioastronomical Institute, University of Bonn, Ed., H. Volland, Bonn, 1994.

Lericos, T.P., H.E. Fuelberg, A.I. Watson, and R.L. Holle, Warm season lightning distributions over the Florida peninsula as related to synoptic patterns, *Wea. and Forecasting*, 17, 83-98, 2002.

Livesey, N.J., M.D. Fromm, J.W. Waters, G.L. Manney, M.L. Santee, and W.G. Read, Enhancement in lower stratospheric CH_3CH observed by the Upper Atmosphere Research Satellite Microwave Limb Sounder following Boreal forest fires, *J. Geophys. Res*., 109, doi:10.1029/2003JD004055, 2004.

Maloney, J.C., H.E. Fuelberg, M.A. Avery, J.H. Crawford, D.R. Blake, B.G. Heikes, G.W. Sachse, S.T. Sandholm, H. Singh, and R.W. Talbot, Chemical characteristics of air from different source regions during the second Pacific Exploratory Mission in the Tropics (PEM-Tropics B), *J. Geophys. Res*., *106*, 32609-32625, 2001.

Martin, B.D., H.E. Fuelberg, N.J. Blake, J.H. Crawford, J.A. Logan, D.R. Blake, and G.W. Sachse, Long range transport of Asian outflow to the equatorial Pacific, *J. Geophys. Res*., 108(D2), 8322, doi:10.1029/2001JD001418, 2002.

McNeal, R.J., J.P. Mugler Jr., R.C. Harriss, and J.M. Hoell Jr., NASA Global Tropospheric Experiment, *Eos Trans. AGU, 64*, 561-562, 1984.

Mauzerall, D.L., J.A. Logan, D.J. Jacob, B.E. Anderson, D. R. Blake, J.D. Bradshaw, B. Heikes, G.W. Sachse, H. Singh, and R. Talbot, Photochemistry in biomass burning plumes and implications for tropospheric ozone over the tropical South Atlantic, *J. Geophys. Res*., *103*, 8401-8423, 1998.

McKeen, S.A. et. al., Ozone production from Canadian wildfires during June and July of 1995, *J. Geophys. Res*., 107, 4192, doi:10.1029/2001JD000697, 2002.

Merrill, J.T., R.E. Newell, and A.S. Bachmeier, A meteorological overview for the Pacific Exploratory Mission-West Phase B, *J. Geophys. Res*., *102*, 28241-28253, 1997.

Morris, G.A., S. Hersey, A.M. Thompson, O.R. Cooper, A. Stohl, P.R. Colarco, W.W. McMillan, J. Warner, B.J. Johnson, J.C. Witte, T.L. Kucsera, D.E. Larko, and S.J. Oltmans, Alaskan and Canadian forest fires exacerbate ozone pollution over Houston, Texas, on 19 and 20 July 2004, *J. Geophys. Res*., 10.1029/2006JD007090, in press, 2006.

Novelli, P.C., K.A. Masarie, P.M. Land, B.D. Hall, R.C. Myers, and J.W. Elkins, Reanalysis of tropospheric CO trends: Effects on the 1997-1998 wildfires, J. *Geophys. Res*., 108, 4464, 2003.

Orville, R.E., and G.R. Huffines, Cloud-to-ground lightning in the United States: NLDN results in the first decade, 1989-1998, *Mon. Wea. Rev*., 129, 1179-1193, 2001.

O'Sullivan, D., B.G. Heikes, M. Lee, W. Chang, G.L. Gregory, D.R. Blake, and G.W. Sachse, Distribution of hydrogen peroxide and methylhydroperoxide over the Pacific and South Atlantic, *J. Geophys. Res*., *104*, 5635-5646, 1999.

Pfister, G., P.G. Hess, L.K. Emmons, J.-F. Lamarque, C. Wiedinmyer, D.P. Edwards, G. Petron, J.C. Gille, and G.W. Sachse, Quantifying CO emissions rom the 2004 Alaskan wildfires using MOPITT CO data, *Geophys. Res. Lett*., 32, L11809, doi:10.1029/2005GL022995, 2005.

Richmond, M.A., and T.L. Shy, An extraordinary summer in the interior of Alaska, 8th Conf. Polar Meteor. and Ocean., Amer. Meteor. Soc., San Diego, Paper P3.24, 2005.

Rozell, N, Smoked pike on menu for Yukon Flats scientists, *Alaska Science Forum*, 1710, 2004.

Russell, P.B., J.M. Livingston, J. Redemann, B. Schmid, S.A. Ramirez, J. Eilers, R. Kahn, A. Chu, L. Remer, P.K. Quinn, M.J. Rood, and W. Wang, Multi-grid-cell validation of satellite aerosol property retrievals in INTEX/ITCT/ICARTT 2004, *J. Geophys. Res*, in press, 2006.

Singh, H. B., W. H. Brune, J. H. Crawford, and D. J. Jacob, Overview of the Summer 2004 Intercontinental Chemical Transport Experiment-North America (INTEX-A), *J. Geophys. Res.,* 2006.

Smith, J.R., H.E. Fuelberg, and A.I. Watson, Warm season lightning distributions over the northern Gulf of Mexico coast and their relation to synoptic scale and mesoscale environments. *Wea. and Forecasting*, 20, 415-438, 2005.

Spichtinger, N., R., Damoah, S. Eckard, C. Forster, P. James, T. Beirle, T. Wagner, P.C. Novelli, and A. Stohl, Boreal forest fires in 1997 and 1998: A seasonal comparison using transport odel simulations and measurement data, *Atmos. Chem Phys.*, 4, 1857-1868, 2004.

Stohl, A., G. Wotawa, P. Seibert, and H. Kromp-Kolb, Interpolation errors in wind fields as a function of spatial and temporal resolution and their impact on different types of kinematic trajectories. *J. Appl. Meteorol., 34*, 2149-2165, 1995.

Stohl, A., Computation, accuracy, and applications of trajectories—A review and bibliography, *Atmos. Environ*., *32*, 947—966, 1998.

Stohl, A., Characteristics of atmospheric transport into the Arctic troposphere, in press, *J. Geophys. Res*., 2006.

Tanimoto, H., Y. Kajii, J. Hirokawa, H. Akimoto, and N.P. Minki, The atmospheric impact of boreal forest fires in far eastern Siberia on the seasonal variation of carbon monoxide: Observations at Richiri, a northern remote island in Japan, *Geophys. Res. Lett*., 27, 4073-4076, 2000.

Tarasick, D.W., et al., Comparison of Canadian air quality forecast models with tropospheric ozone profile measurements above mid-latitude North America during the IONS/ICARTT campaign: Evidence for stratospheric input, *J. Geophys. Res*., 2006.

Thompson A.M., et al., Stratospheric contributions to tropospheric ozone profiles in eastern North America, July-August 2004 (IONS): A typical "spring-like summer?", *J. Geophys. Res*., 2006.

Trenberth, K.E., Short-term climate variations: Recent accomplishments and issues for future progress, *Bull. Am. Meteorol. Soc., 78*, 1081-1096, 1997.

Turquety, S., et al., Inventory of boreal fire emissions for North America: Importance of peat burning and pyro-convective injection, *J. Geophys. Res*., 2006.

Wilks, D.S., *Statistical Methods in the Atmospheric Sciences*, 2nd ed., Academic Press, pp 73-76, 2006.

Wotawa, G., and M. Trainer, The influence of Canadian forest fires on pollutant concentrations in the United States, *Science*, 288, 324-328, 2000.

Wotawa, G., P.C. Novelli, M. Trainer, and C. Granier, Inter-annual variability of summertime CO concentrations in the Northern Hemisphere explained by boreal forest forest in North America and Russia, *Geophys. Res. Lett*., 28, 4575-4578, 2001.

Yurganov, N.L., T. Blumenstock, I.E. Grechko, F. Hase, J.E. Hyer, E.S. Kasischke, M. Koike, Y. Kondo, I. Kramer, F.-Y. Leung, E. Mahiau, J. Mellqvist, J. Notholt, C. Novelli, P.C. Rinsland, E.H. Scheel, A. Schulz, A. Strandberg, R. Sussmann, H. Tanimoto, V. Velazco, R. Zander, and Y. Zhao, A quantitative assessment of the 1998 carbon monoxide emissions anomaly in the Northern Hemisphere based on total column and surface concentration measurements, *J. Geophys. Res*., 109, doi:10.1029/2004JD004559, 2004.

Figure Captions

Figure 1 Mean conditions during the INTEX-NA period (July 1 – August 15, 2004) and departures from the long-term climatology. Panels a) - c) are, respectively, mean vector winds and isotachs at 250 hPa (~34,000 ft), mean geopotential height pattern at 500 hPa (~18,000 ft), and mean sea level pressure (hPa). Panels d) – f) depict departures of the INTEX-NA period from the long-term climatology. The data were provided by the NOAA-CIRES Climate Diagnostics Center, Boulder Colorado from their Web site at http://www.cdc.noaa.gov/.

Figure 2 Geopotential height patterns at 500 hPa (~ 18,000 ft) for selected days during INTEX-NA. The data were provided by the NOAA-CIRES Climate Diagnostics Center, Boulder Colorado from their Web site at http://www.cdc.noaa.gov/.

Figure 3 Time vs longitude (Hűvmuller) diagram of 500 hPa mean geopotential height at 40^{o}N. The data were provided by the NOAA-CIRES Climate Diagnostics Center, Boulder Colorado from their Web site at http://www.cdc.noaa.gov/

Figure 4 Mean geopotential heights at 500 hPa (~18,000 ft) for the periods a) July 1 – July 14, 2004 and c) July 15 – August 15, 2004. Panels b) and d) are anomalies of these means from the long-term climatology. The data were provided by the NOAA-CIRES Climate Diagnostics Center, Boulder Colorado from their Web site at http://www.cdc.noaa.gov/

Figure 5 Surface analyses for a) July 20, b) July 25, c) August 2, d) August 6, and e) August 15 prepared by the National Weather Service. Analyses are from the NOAA

Central Library Data Imaging Project from their Web site at http://docs.lib.noaa.gov/rescue/dwm/data_rescue_daily_weather_maps.html

Figure 6 MODIS images showing wildfire locations and smoke plumes over a) Alaska and northwestern Canada on July 1, 2004, and b) northwest Canada on July 25, 2004. Images were provided by NASA at http://earthobservatory.nasa.gov/NaturalHazards.

Figure 7 MODIS images showing smoke plumes over a) the Labrador Sea off the coast of Newfoundland on July 19, 2004, and b) southeast Texas and coastal Louisiana on July 19, 2004. Images were provided by NASA at http://earthobservatory.nasa.gov/NaturalHazards

Figure 8 Horizontal and vertical plots of backward trajectories from three legs of the DC-8 flight on July 18, 2004 when a biomass burning plume was encountered over the Labrador Sea, a) 10 days back arriving at the DC-8 near 500 hPa, b) 7 days back arriving at the DC-8 near 300 hPa, and c) 5 days back arriving at the DC-8 between 500 and 300 hPa (~18,000 ft – 30,000 ft). The Florida State archive of INTEX-NA trajectory plots is available on the Web at http://fuelberg.met.fsu.edu/research/intexa.

Figure 9 Photos taken from the cockpit of the DC-8 by the lead author during the flight on July 20, 2004 as the aircraft was approaching Portsmouth, NH. Panel a) shows the plume ahead of a developing cumulus cloud, while panel b) shows the northeastern edge of the plume. Note the thick and several thin layers of pollution in panel a).

Figure 10 Horizontal and vertical plots of 7 day backward trajectories arriving at the DC-8 at the location of the observed plume in Figure 9. The trajectories arrive at the height of the aircraft (~ 600 hPa, ~14,000 ft). Note the trajectory origins over the wildfire regions of Alaska.

Figure 11 Photos taken from the cockpit of the DC-8 by the lead author showing inter-comparison flights with a) the NOAA P-3B aircraft on August 7, 2004 and b) the British Bae-146 aircraft on July 28, 2004.

Figure 12 Horizontal and vertical of plots of 7 day forward trajectories beginning on July 18, 2004 from flight legs shown in Figure 10.

Figure 13 Flash densities of cloud-to-ground lightning during the complete INTEX-NA period between July 1 – August 15, 2004. Flashes are counted within boxes that are 11 km on each side.

Figure 14 Daily counts of cloud-to-ground lightning within the area 66^{o}W-126^{o}W, 25^{o}N-50^{o}N. Day 1 denotes July 1, 2004.

Figure 15 Photo taken from the cockpit of the DC-8 by the lead author showing nearby intense deep convection on July 20, 2004.

Figure 16 a) GOES infrared image at 1945 UTC July 12, 2004 (Flight 7). The flight track of the DC-8 is superimposed, where the different colors represent hourly locations of the aircraft. The images are courtesy of David Westberg.

b) As in panel a) but for 1732 UTC July 25, 2004 (Flight 12).

Figure 17 Locations where backward trajectories from the DC-8 at 1 min intervals intercepted cloud-to-ground lightning flashes between July 9 – July 12, 2004. At least one NLDN flash had to occur within a 1 deg radius and 1 h window of the trajectory to be included. The various colors represent the hours back from the flight track before the lightning encounter. The DC-8 flight track and its altitude on July 12 are superimposed along with streamlines of the flow at 500 hPa.

Table 1. Number of cold fronts passing Boston and Atlanta between July 1 – August 15 in the years 2000 - 2004. The average time (days) between frontal passages at Boston also is given. Frontal locations were obtained from the National Weather Service's archive of Daily Weather Maps http://docs.lib.noaa.gov/rescue/dwm/data_rescue_daily_weather_maps.html.

Year	Cold Fronts passing Boston	Avg. Time between passages (days)	Cold Fronts passing Atlanta
2000	5	9.0	4
2001	7	6.6	5
2002	8	4.6	3
2003	7	5.8	5
2004	9	4.6	7
2005	12	4.0	3

Table 2. Cloud-to-ground lightning flashes within the area 66°W-126°W, 25°N-50°N during the 6 week INTEX-A period (July 1 – August 15). Flashes less than 15 kA are not included since they are believed to represent intra-cloud discharges [*K. Cummins*, Vaisala Inc., personal communication]

Year	July 1-31	August 1-15	July 1-August 15
2003	7,329,890	3,549,906	10,879,796
2004	7,691,566	3,001,042	10,692,608
2005	6,873,867	3,871,840	10,745,707

Table 3. Percentage of trajectories for all INTEX flights combined that encountered either convection (Conv) based on GFS analysis data, the planetary boundary layer (PBL), the residual layer (RL), the stratosphere (strat), or lightning based on either 1 or 60 NLDN-derived flashes within 0.5 or 1.5 deg lat. between 6 hours and 240 hours (10 days) before in situ sampling by the DC-8. Once a trajectory encountered one of these conditions subsequent encounters within the same category were not counted.

Time back, (hours)	Convection From GFS Analyses	PBL	Residual Layer	Strat.	Over Land	Lightning 1 NLDN 0.5 deg	Lightning 1 NLDN 1.5deg	Lightning 60NLDN 0.5 deg	Lightning 60NLDN 1.5 deg
6	21.4%	20.5%	11.4%	5.5%	69.4%	8.2%	17.7%	2.4%	7.9%
12	9.1%	0.5%	7.3%	2.0%	5.1%	4.8%	8.2%	1.6%	4.0%
18	9.3%	2.3%	2.4%	1.6%	4.2%	6.4%	9.5%	2.6%	6.6%
24	6.6%	2.2%	1.3%	1.9%	3.2%	6.1%	6.7%	3.3%	6.1%
36	9.9%	1.3%	3.7%	2.4%	3.4%	5.4%	5.5%	3.1%	4.6%
48	7.0%	4.0%	2.4%	1.7%	2.1%	7.8%	9.1%	4.2%	8.1%
60	4.4%	1.1%	2.9%	2.1%	1.4%	4.0%	2.5%	2.9%	3.8%
72	3.7%	2.9%	2.0%	1.3%	0.9%	4.0%	2.7%	3.0%	4.0%
96	6.3%	2.9%	4.0%	1.8%	1.1%	2.7%	2.2%	2.9%	2.3%
120	3.5%	2.4%	2.6%	1.6%	0.9%	1.7%	1.1%	1.9%	1.7%
144	2.9%	1.9%	2.0%	1.0%	0.8%	1.0%	0.5%	1.4%	0.9%
168	2.5%	1.7%	2.2%	1.5%	0.3%	0.5%	0.4%	0.5%	0.4%
192	2.1%	2.1%	2.2%	1.1%	0.3%	0.6%	0.4%	0.5%	0.5%
216	2.1%	1.6%	1.7%	1.0%	0.4%	0.2%	0.4%	0.5%	0.3%
240	1.0%	1.0%	1.0%	0.9%	0.1%	0.1%	0.2%	0.2%	0.1%
No Influence	8.3%	51.4%	50.9%	72.7%	6.5%	46.4%	32.9%	69.0%	48.8%

Table 4. Percentage of trajectories' first encounter with convection during INTEX-A along with the first convective encounter due to random chance.

Time back (hours)	Convection by chance	GFS-derived convection
6	12.5%	21.4%
12	10.9%	9.1%
18	9.6%	9.3%
24	8.4%	6.6%
36	13.7%	9.9%
48	10.5%	7.0%
60	8.1%	4.4%
72	6.2%	3.7%
96	8.3%	6.3%
120	4.9%	3.5%
144	2.9%	2.9%
168	1.7%	2.5%
192	1.0%	2.1%
216	0.6%	2.1%
240	0.3%	1.0%
No Influences	0.5%	8.3%

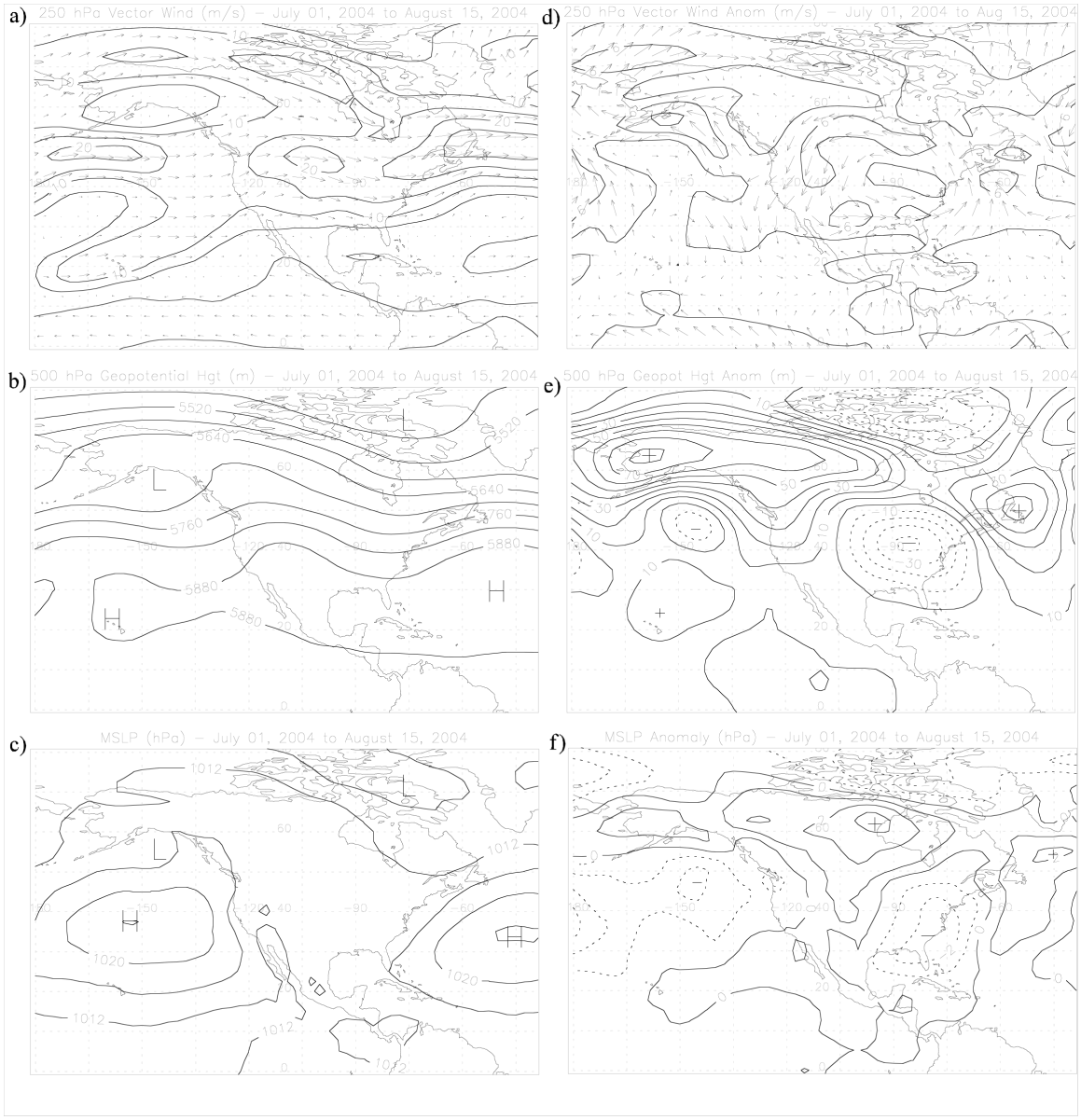

Figure 1 Mean conditions during the INTEX-NA period (July 1 – August 15, 2004) and departures from the long-term climatology. Panels a) - c) are, respectively, mean vector winds and isotachs at 250 hPa (~34,000 ft), mean geopotential height pattern at 500 hPa (~18,000 ft), and mean sea level pressure (hPa). Panels d) – f) depict departures of the INTEX-NA period from the long-term climatology. The data were provided by the NOAA-CIRES Climate Diagnostics Center, Boulder Colorado from their Web site at http://www.cdc.noaa.gov/.

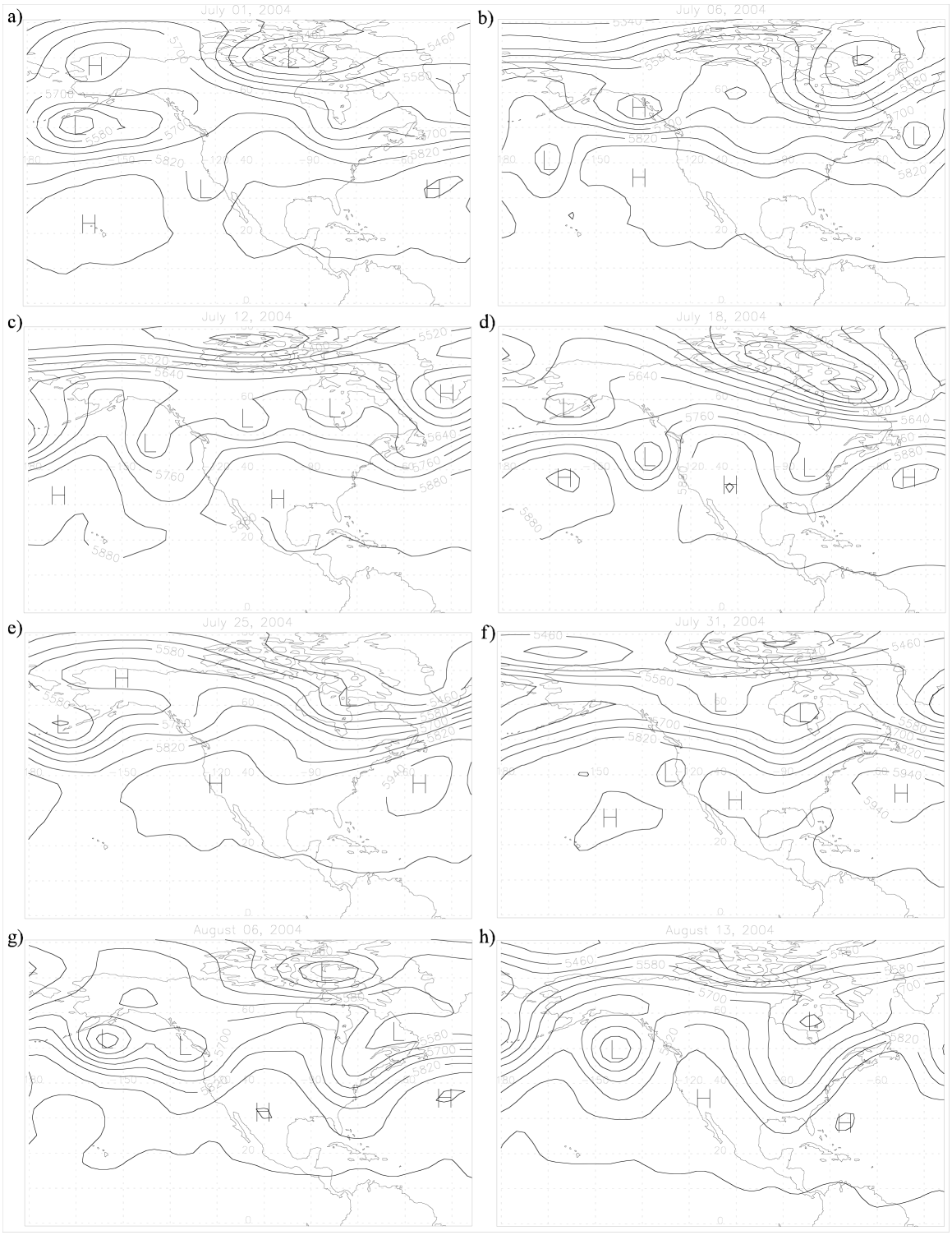

Figure 2 Geopotential height patterns at 500 hPa (~ 18,000 ft) for selected days during INTEX-NA. The data were provided by the NOAA-CIRES Climate Diagnostics Center, Boulder Colorado from their Web site at http://www.cdc.noaa.gov/.

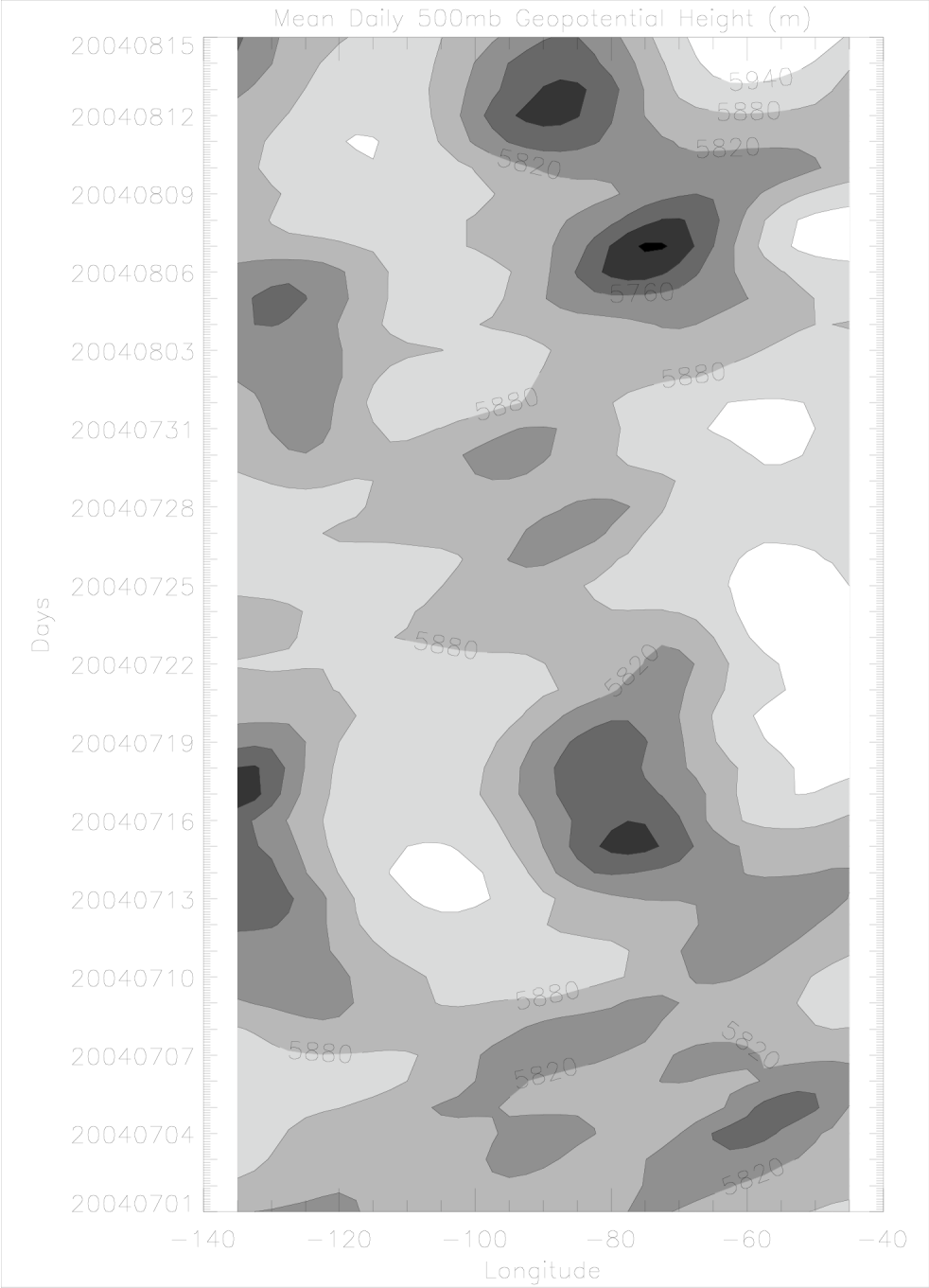

Figure 3 Time vs longitude (Hűvmuller) diagram of 500 hPa mean geopotential height at 40°N. The data were provided by the NOAA-CIRES Climate Diagnostics Center, Boulder Colorado from their Web site at http://www.cdc.noaa.gov/

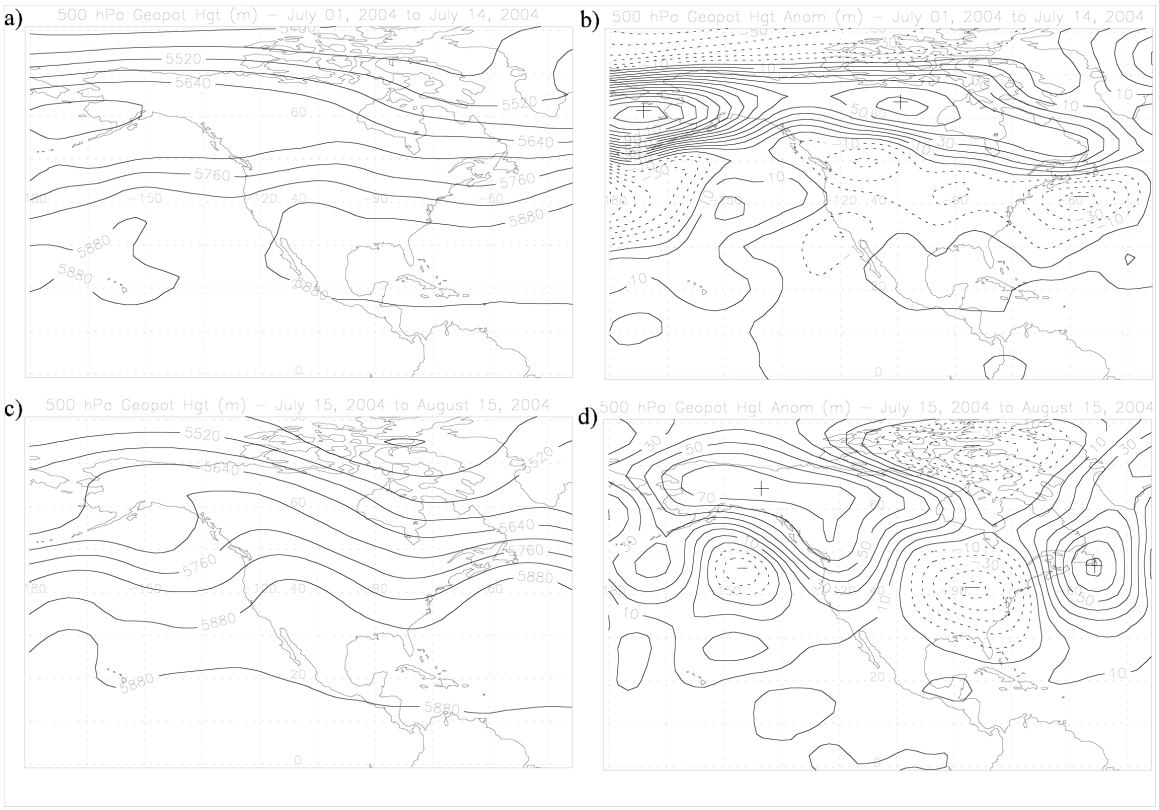

Figure 4 Mean geopotential heights at 500 hPa (~18,000 ft) for the periods a) July 1 – July 14, 2004 and c) July 15 – August 15, 2004. Panels b) and d) are anomalies of these means from the long-term climatology. The data were provided by the NOAA-CIRES Climate Diagnostics Center, Boulder Colorado from their Web site at http://www.cdc.noaa.gov/

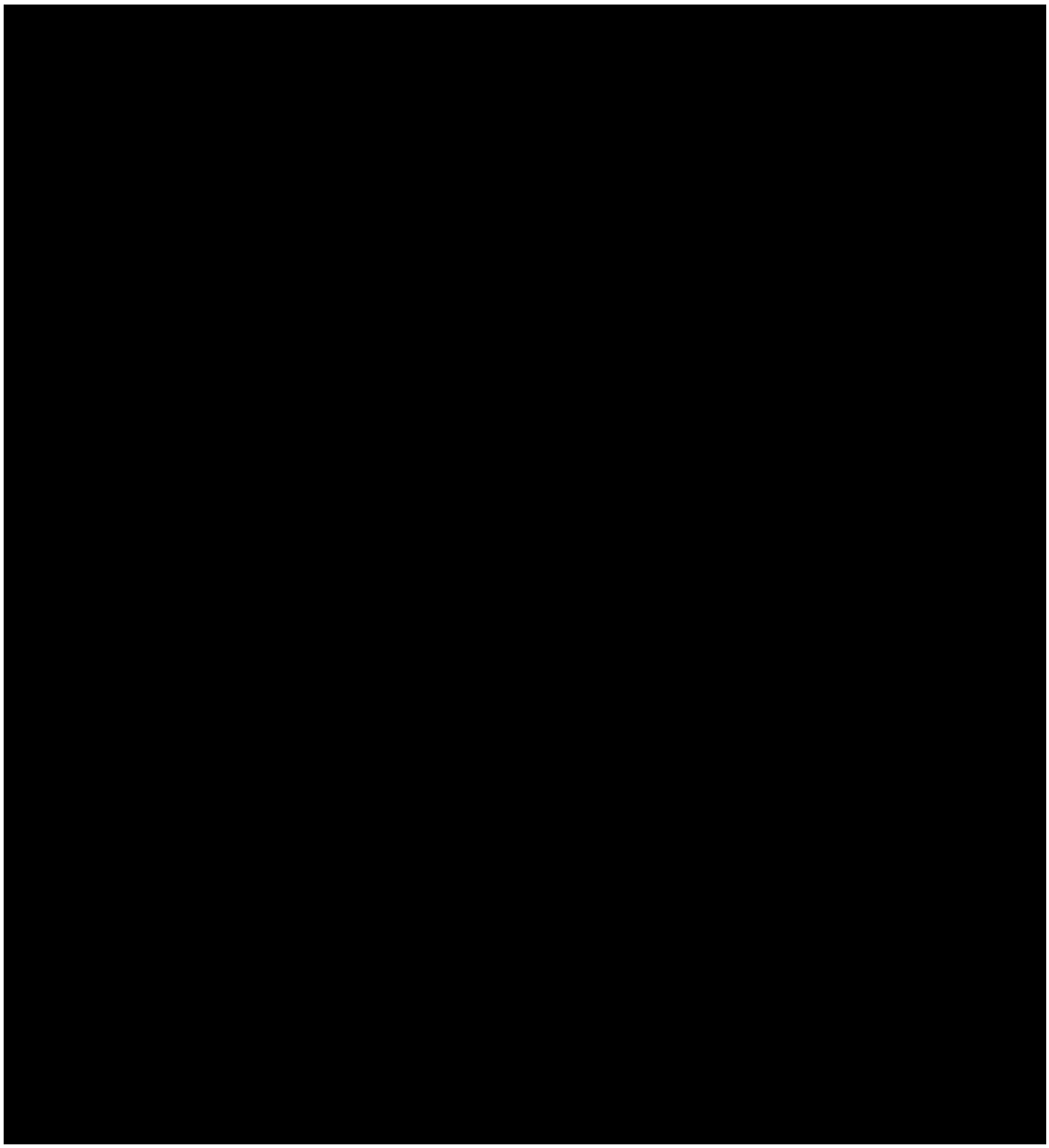

Figure 5 Surface analyses for a) July 20, b) July 25, c) August 2, d) August 6, and e) August 15 prepared by the National Weather Service. Analyses are from the NOAA Central Library Data Imaging Project from their Web site at http://docs.lib.noaa.gov/rescue/dwm/data_rescue_daily_weather_maps.html

a)

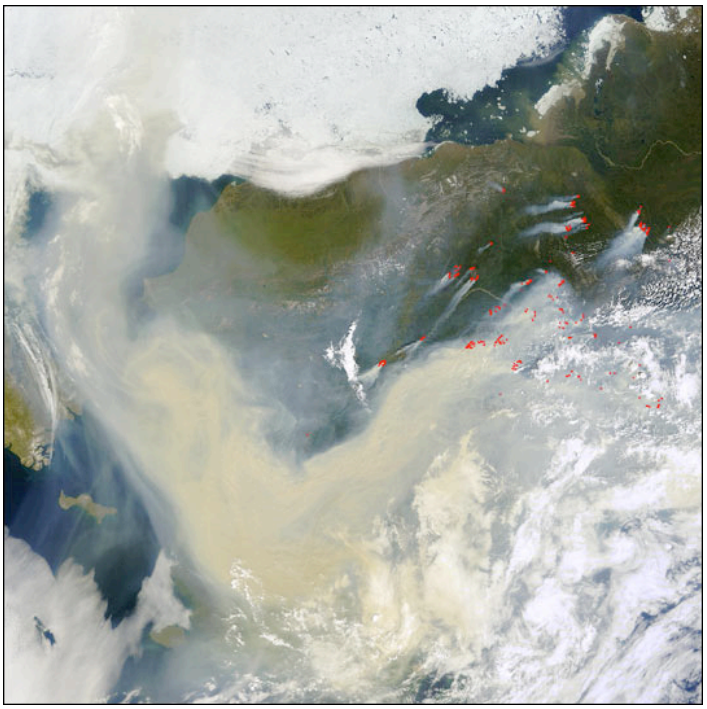

b)

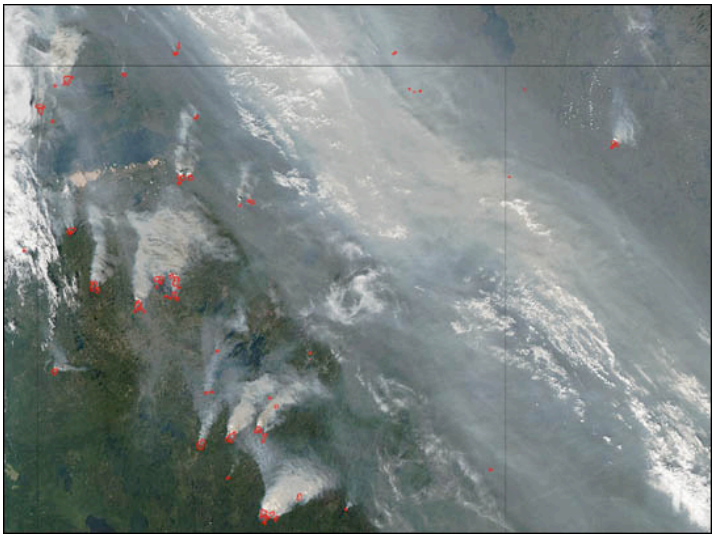

Figure 6 MODIS images showing wildfire locations and smoke plumes over a) Alaska and northwestern Canada on July 1, 2004, and b) northwest Canada on July 25, 2004. Images were provided by NASA at http://earthobservatory.nasa.gov/NaturalHazards

a)

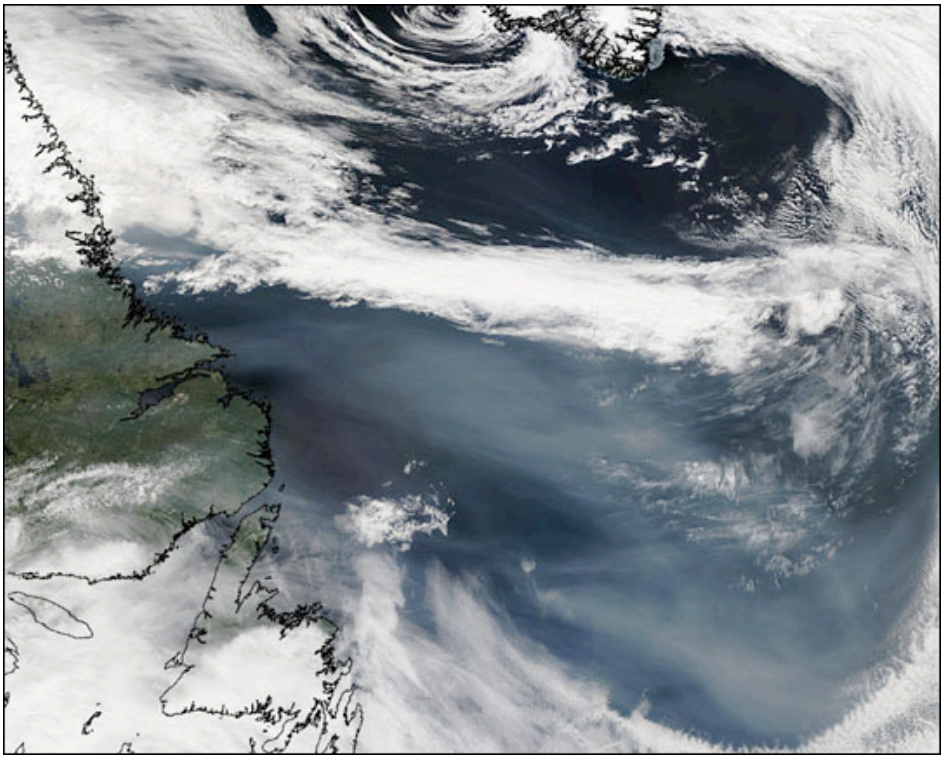

b)

Figure 7 MODIS images showing smoke plumes over a) the Labrador Sea off the coast of Newfoundland on July 19, 2004, and b) southeast Texas and coastal Louisiana on July 19, 2004. Images were provided by NASA at http://earthobservatory.nasa.gov/NaturalHazards

a)

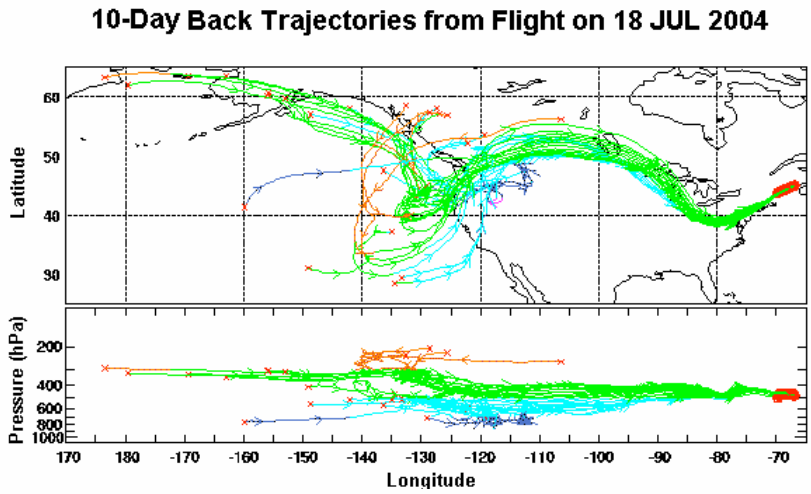

b)

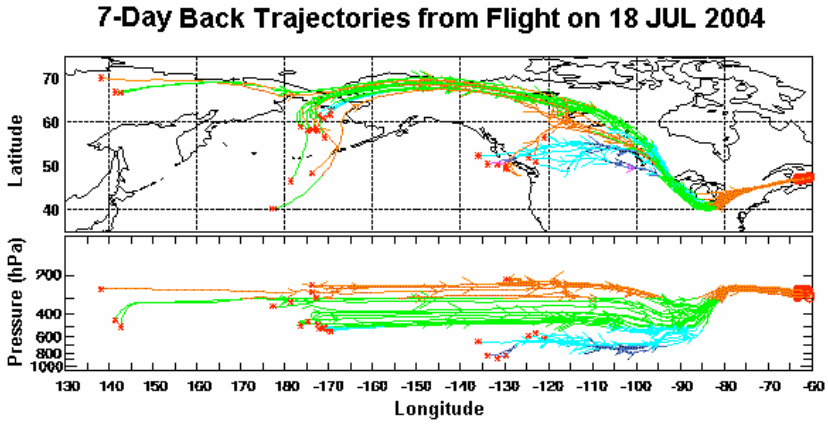

c)

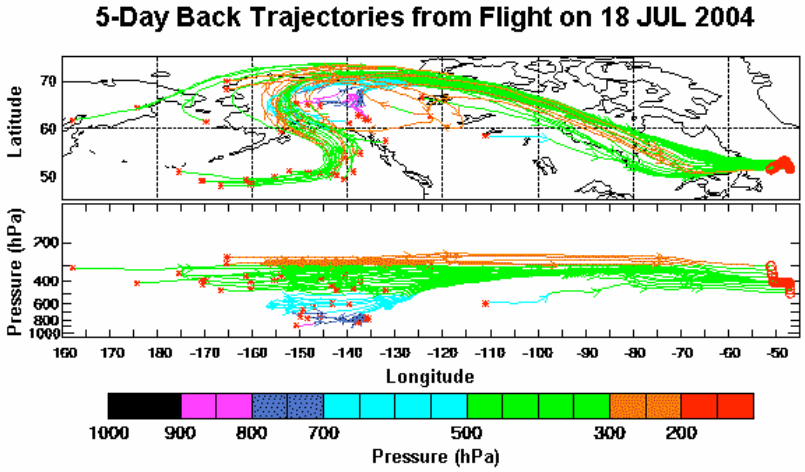

Figure 8 Horizontal and vertical plots of backward trajectories from three legs of the DC-8 flight on July 18, 2004 when a biomass burning plume was encountered over the Labrador Sea, a) 10 days back arriving at the DC-8 near 500 hPa, b) 7 days back arriving at the DC-8 near 300 hPa, and c) 5 days back arriving at the DC-8 between 500 and 300 hPa (~18,000 ft – 30,000 ft). The Florida State archive of INTEX-NA trajectory plots is available on the Web at http://fuelberg.met.fsu.edu/research/intexa/.

a)

b)

Figure 9 Photos taken from the cockpit of the DC-8 by the lead author during the flight on July 20, 2004 as the aircraft was approaching Portsmouth, NH. Panel a) shows the plume ahead of a developing cumulus cloud, while panel b) shows the northeastern edge of the plume. Note the thick and several thin layers of pollution in panel a).

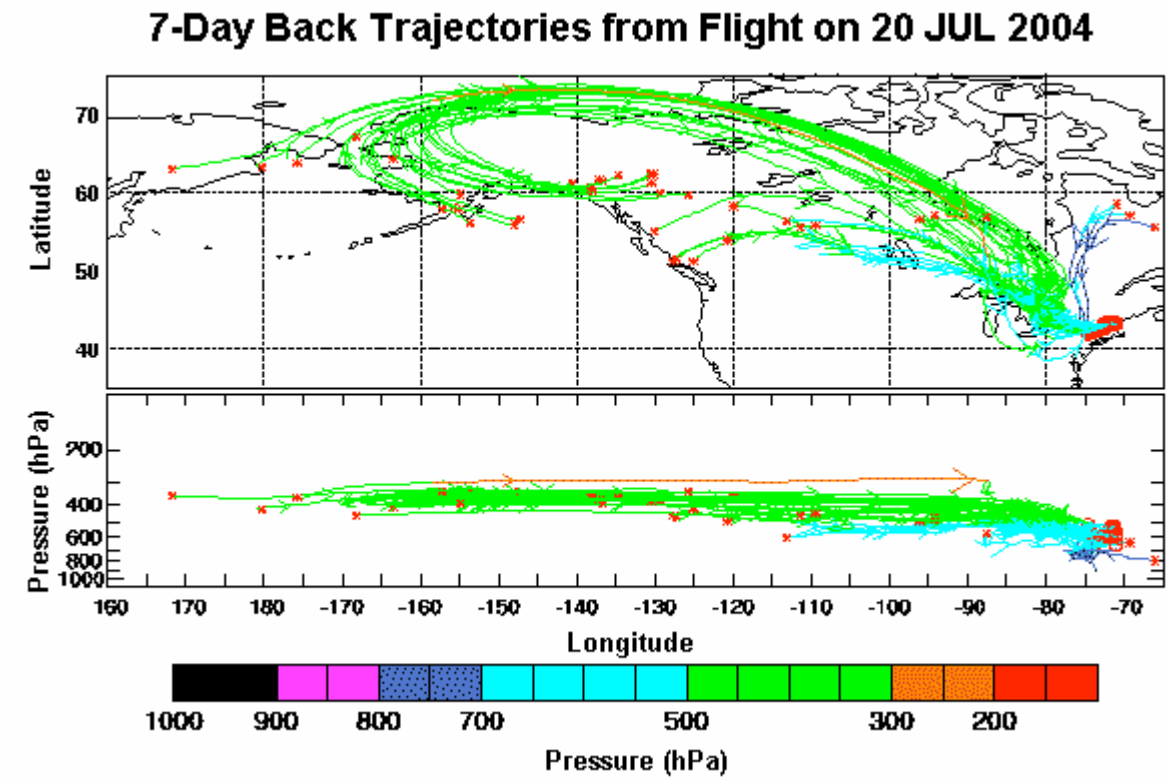

Figure 10 Horizontal and vertical plots of 7 day backward trajectories arriving at the DC-8 at the location of the observed plume in Figure 9. The trajectories arrive at the height of the aircraft (~ 600 hPa, ~14,000 ft). Note the trajectory origins over the wildfire regions of Alaska.

a)

b)

Figure 11 Photos taken from the cockpit of the DC-8 by the lead author showing inter-comparison flights with a) the NOAA P-3B aircraft on August 7, 2004 and b) the British Bae-146 aircraft on July 28, 2004.

a)

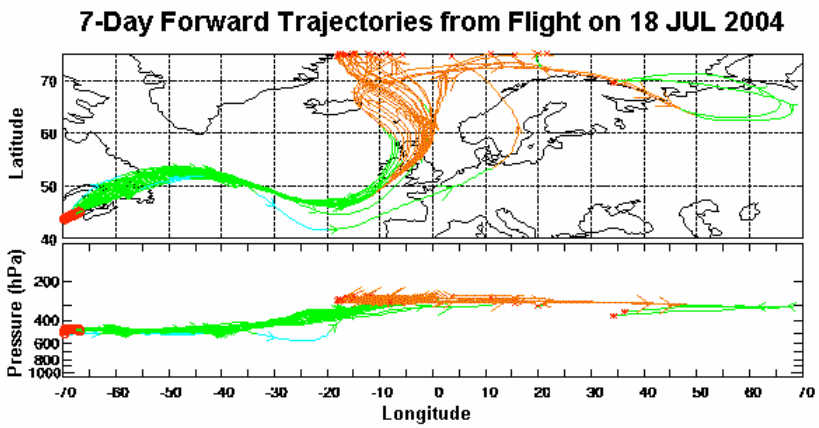

b)

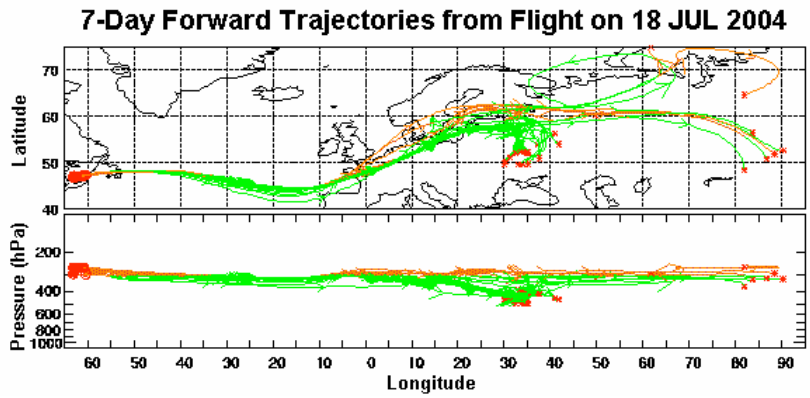

c)

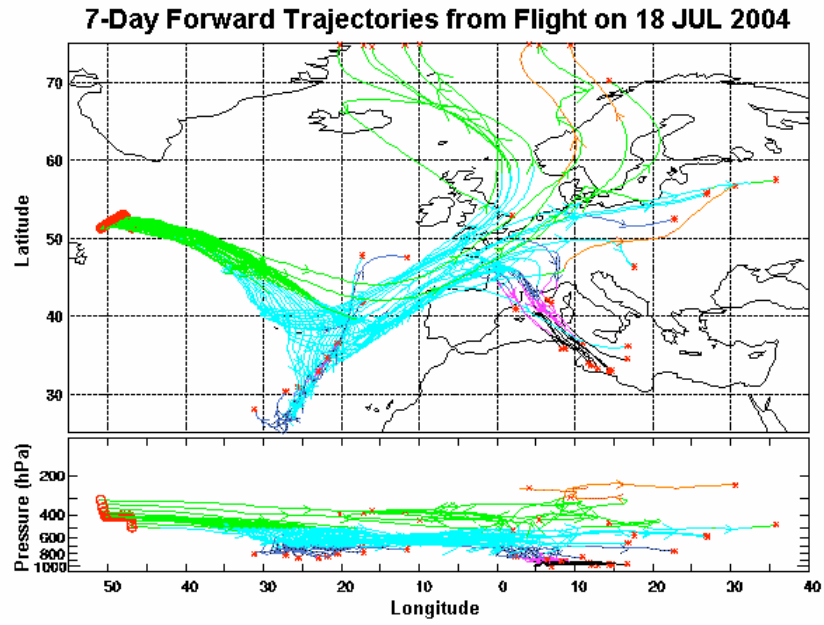

Figure 12 Horizontal and vertical of plots of 7 day forward trajectories beginning on July 18, 2004 from flight legs shown in Figure 10.

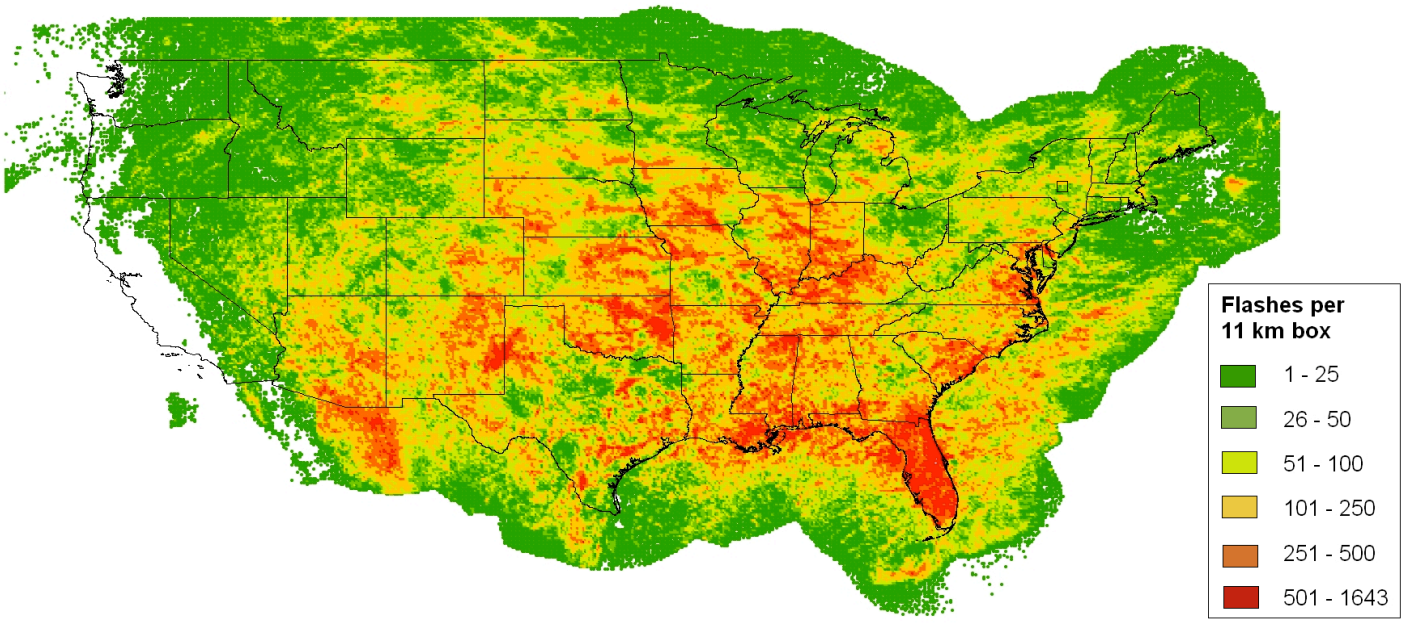

Figure 13 Flash densities of cloud-to-ground lightning during the complete INTEX-NA period between July 1 – August 15, 2004. Flashes are counted within boxes that are 11 km on each side.

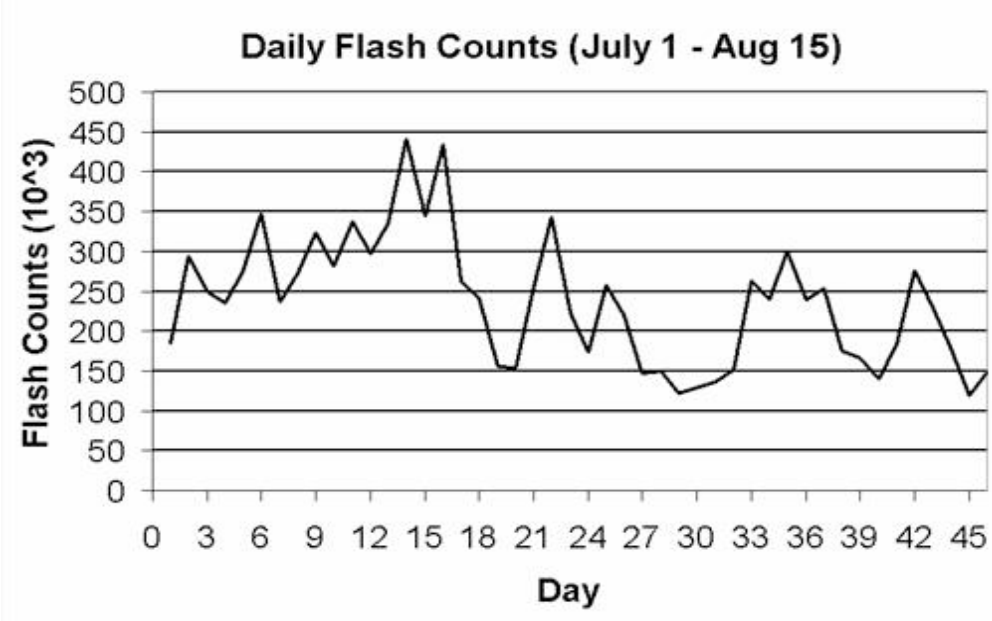

Figure 14 Daily counts of cloud-to-ground lightning within the area 66°W-126°W, 25°N-50°N. Day 1 denotes July 1, 2004.

Figure 15 Photo taken from the cockpit of the DC-8 by the lead author showing nearby intense deep convection on July 20, 2004.

a)

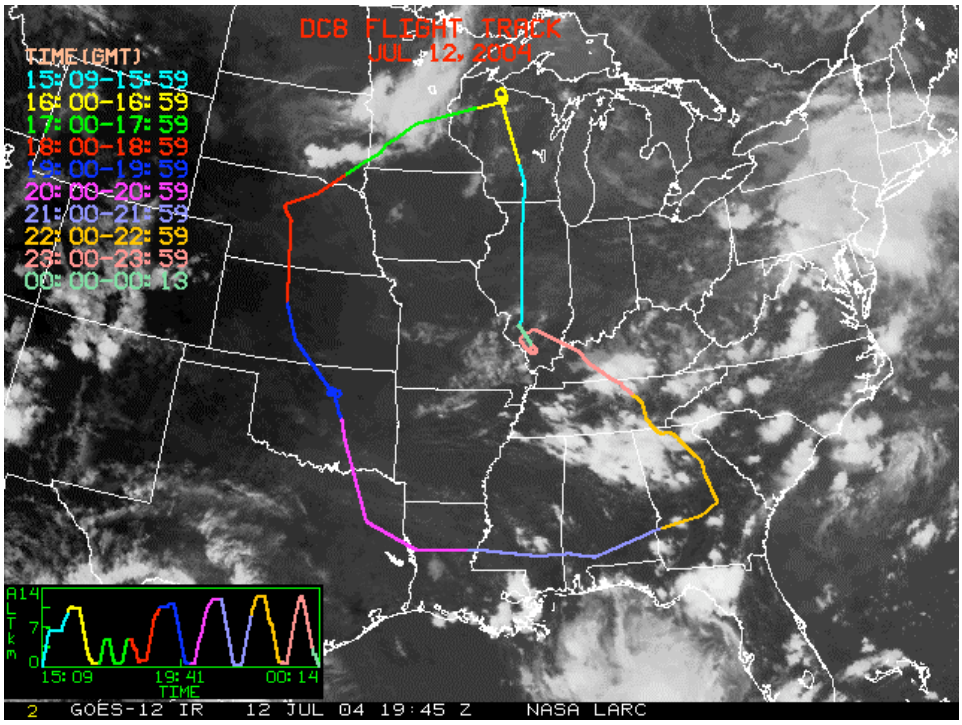

b)

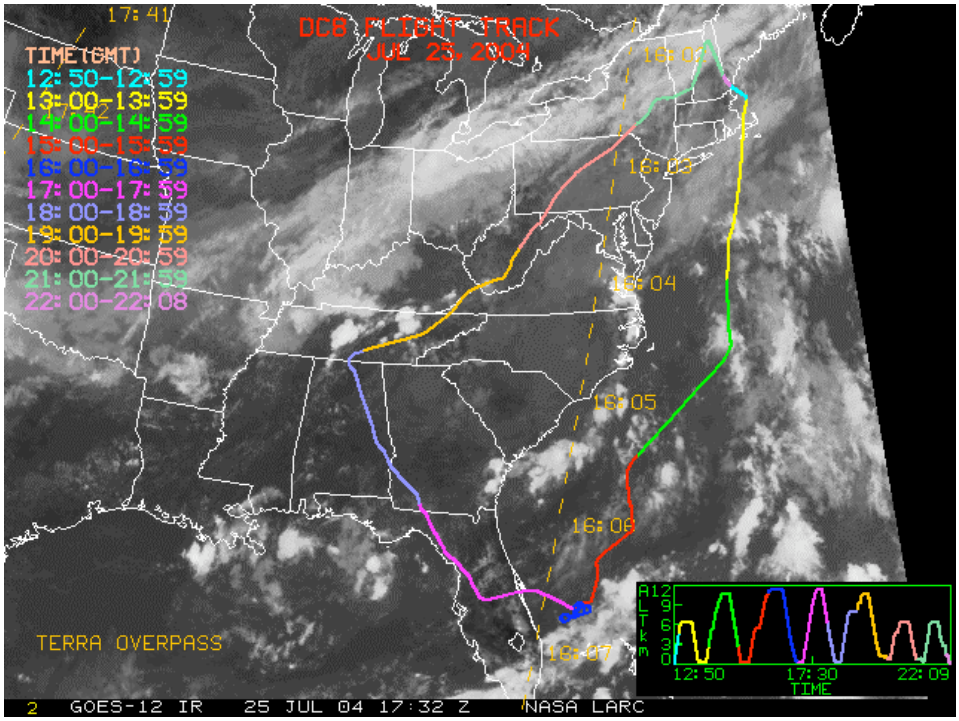

Figure 16 a) GOES infrared image at 1945 UTC July 12, 2004 (Flight 7). The flight track of the DC-8 is superimposed, where the different colors represent hourly locations of the aircraft. The images are courtesy of David Westberg.

b) As in panel a) but for 1732 UTC July 25, 2004 (Flight 12).

a)

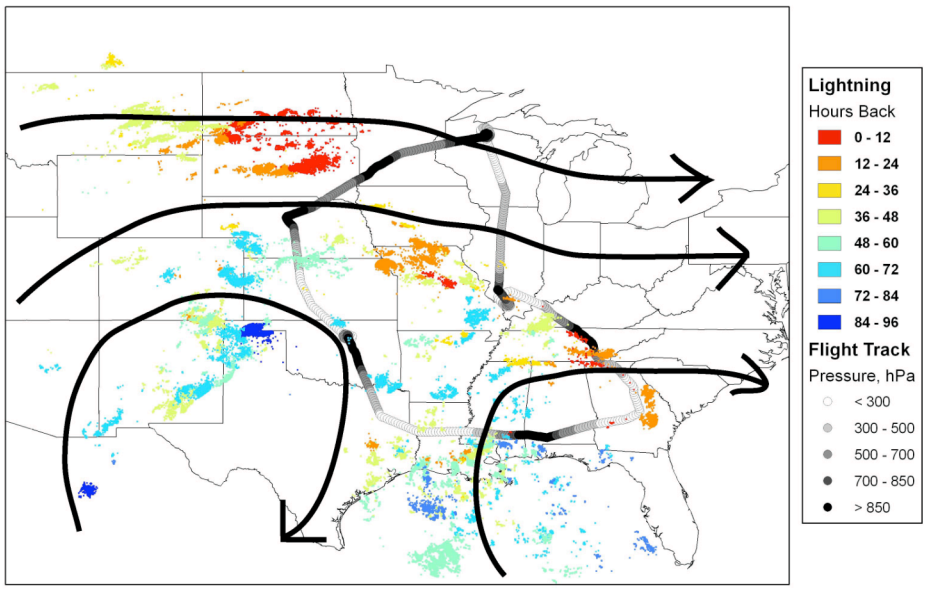

b)

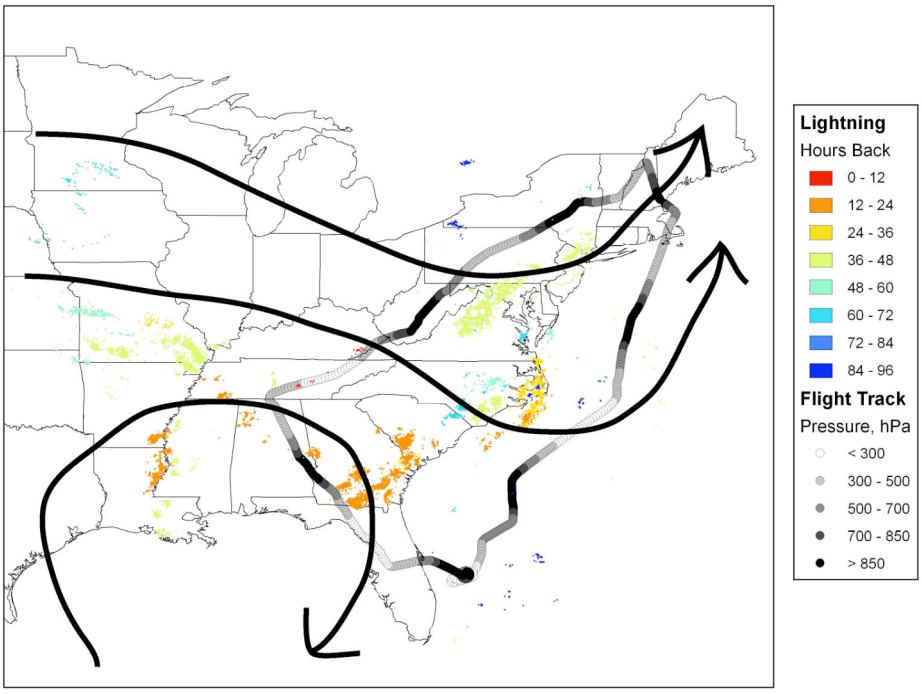

Figure 17 Locations where backward trajectories from the DC-8 at 1 min intervals intercepted cloud-to-ground lightning flashes between a) July 9 – July 12, 2004 and b) July 22 – July 25, 2004 . At least one NLDN flash had to occur within a 1 deg radius and 1 h window of the trajectory to be included. The various colors represent the hours back from the flight track before the lightning encounter. The DC-8 flight track and its altitude on a) July 12 and b) July 25 are superimposed along with streamlines of the flow at 500 hPa.